The Journal of Comparative Neurology Research in Systems Neuroscience

THE JOURNAL OF COMPARATIVE NEUROLOGY 384:597–620 (1997)

Neurofilament and Calcium-Binding Proteins in the Human Cingulate Cortex

ESTHER A. NIMCHINSKY,[1] BRENT A. VOGT,[4] JOHN H. MORRISON,[1,2] AND PATRICK R. HOF[1,2,3]*

[1]Fishberg Research Center for Neurobiology and Neurobiology of Aging Laboratories, Mount Sinai School of Medicine, New York, New York 10029

[2]Department of Geriatrics and Adult Development, Mount Sinai School of Medicine, New York, New York 10029

[3]Department of Ophthalmology, Mount Sinai School of Medicine, New York, New York 10029

[4]Department of Physiology and Pharmacology, Bowman Gray School of Medicine, Wake Forest University, Winston-Salem, North Carolina 27157

ABSTRACT

Functional imaging studies of the human brain have suggested the involvement of the cingulate gyrus in a wide variety of affective, cognitive, motor, and sensory functions. These studies highlighted the need for detailed anatomic analyses to delineate its many cortical fields more clearly. In the present study, neurofilament protein, and the calcium-binding proteins parvalbumin, calbindin, and calretinin were used as neurochemical markers to study the differences among areas and subareas in the distributions of particular cell types or neuropil staining patterns. The most rostral parts of the anterior cingulate cortex were marked by a lower density of neurofilament protein-containing neurons, which were virtually restricted to layers V and VI. Immunoreactive layer III neurons, in contrast, were sparse in the anterior cingulate cortex, and reached maximal densities in the posterior cingulate cortex. These neurons were more prevalent in dorsal than in ventral portions of the gyrus. Parvalbumin-immunoreactive neurons generally had the same distribution. Calbindin- and calretinin-immunoreactive nonpyramidal neurons had a more uniform distribution along the gyrus. Calbindin-immunoreactive pyramidal neurons were more abundant anteriorly than posteriorly, and a population of calretinin-immunoreactive pyramidal-like neurons in layer V was found largely in the most anterior and ventral portions of the gyrus. Neuropil labeling with parvalbumin and calbindin was most dense in layer III of the anterior cingulate cortex. In addition, parvalbumin-immunoreactive axonal cartridges were most dense in layer V of area 24a. Calretinin immunoreactivity showed less regional specificity, with the exception of areas 29 and 30. These chemoarchitectonic features may represent cellular reflections of functional specializations in distinct domains of the cingulate cortex. J. Comp. Neurol. 384:597–620, 1997. © 1997 Wiley-Liss, Inc.

Indexing terms: calbindin; calretinin; cerebral cortex; human brain chemoarchitecture; limbic system; parvalbumin

The diverse cytoarchitecture of the human cingulate cortex has been assessed with Nissl-stained preparations for almost a century. The early works of Brodmann (1909) and Von Economo (1927) demonstrated that the human cingulate cortex has a primary border between agranular anterior and granular posterior regions that are referred to as areas 24/23 and LA/LC, respectively, by these authors. Von Economo (1927) further divided these regions of the cingulate gyral surface into three regions in the dorsoventral axis, and Rose (1927) provided a very elaborate parcellation of anterior cingulate cortex. These early observations, however, did not fit well with a growing body of evidence about the neurobiology of cingulate cortex and required a number of modifications. Important new findings include the observation of a gigantopyramidal field in the depths of the cingulate sulcus by using pigmentoarchi-

Grant sponsor: NIH; Grant number: AG05138, AG11480, and the Human Brain Project MHDA52154; Grant sponsor: the Brookdale Foundation.

*Correspondence to: Dr. Patrick R. Hof, Neurobiology of Aging Laboratories, Box 1639, Mount Sinai School of Medicine, One Gustave L. Levy Place, New York, NY 10029. E-mail: hof@cortex.neuro.mssm.edu

Received 22 December 1996; Revised 24 March 1997; Accepted 26 March 1997

tecture (Braak, 1976; Braak and Braak, 1976). This area is now known to contain corticospinal projection neurons (Dum and Strick, 1991, 1992, 1993), and projections to the motor cortex (Morecraft and Van Hoesen, 1992; Nimchinsky et al., 1996). Braak (1979b) also observed a magnocellular division of the perigenual cortex suggesting that there may be rostral and caudal subdivisions of Brodmann's area 24. Finally, a thorough modification of Brodmann's original scheme has been made that includes Braak's observations as well as those made in macaque monkey cingulate cortex based on the connections of anterior and posterior area 24 (Vogt et al., 1995). This latter analysis of the human cingulate cortex was presented in flat map format and shows the full extent of many more cytoarchitectural areas then were originally described by Brodmann (1909).

In the human and the nonhuman primate, the most obvious distinction is that the anterior portion of the cingulate gyrus, dorsal to the corpus callosum, lacks a layer IV, and is designated area 24, distinguishing it from the posterior portion of the gyrus, area 23, which does have a layer IV (Vogt et al., 1995). More subtle differences in cortical architecture, such as the relative prominence of layer II, the thickness of layer III, and the width, sublayering, and cellular composition of layer V, help to divide further these areas into consecutive strips of cortex beginning close to the depth of the callosal sulcus with area 24a and 23a (in the anterior and posterior parts of the cingulate gyrus, respectively), continuing onto the medial wall of the gyrus (24b and 23b), and extending to or even dorsal to the depth of the cingulate sulcus (24c and 23c; Vogt et al., 1987, 1995; Vogt, 1993). The transition from anterior to posterior cingulate cortex is not an abrupt one, and occupies a distinct cortical area designated 24′, which is also subdivided in the ventrodorsal direction into areas 24a′, 24b′, and 24c'. The cortical areas that lie immediately rostral and ventral to the genu of the corpus callosum are also considered part of the cingulate cortex, and are designated areas 32 and 25, respectively (Vogt et al., 1987, 1995; Vogt, 1993). Finally, a cytoarchitectonically distinctive complex of cortical areas that lie caudally in the depth of the callosal sulcus, laterally to area 23a, is designated area 29, which is subdivided into areas 29a–d, and area 30, which is located between area 29 and 23a (Vogt et al., 1987, 1995; Vogt, 1993).

Although Nissl stained preparations continue to be useful to parcellate this region, immunohistochemical analyses of the distribution of several neuronal markers show that many of these areas have phenotypical differences. Used jointly, they provide a more complete picture of the different areas within the cingulate cortex. One such marker is neurofilament protein, which has been visualized immunocytochemically by using an antibody that recognizes a nonphosphorylated epitope on the neurofilament protein triplet (Sternberger and Sternberger, 1983; Lee et al., 1988). Neurofilament protein is found in a subpopulation of cortical neurons that vary in their distribution in different regions of the cerebral cortex (Campbell and Morrison, 1989; Hof and Morrison, 1995; Hof et al., 1995a). A recent study in the macaque monkey showed that systematic variation in the distribution of neurofilament protein could be used to identify all cytoarchitecturally defined visual areas, including many cortical regions whose boundaries are not readily discernable on the basis of the Nissl stain (Hof and Morrison, 1995). Another study used this marker to delineate chemoarchitectural subdivisions of the human orbitofrontal cortex (Hof et al., 1995a). Additionally, this marker has been shown to be a reliable chemoarchitectonic indicator of the cingulate motor areas in the macaque monkey (Nimchinsky et al., 1996).

Another set of useful markers are the calcium-binding proteins parvalbumin, calbindin, and calretinin. With the exception of a population of pyramidal neurons that contain calbindin, the neurons that contain these proteins are GABAergic interneurons (Celio, 1990; DeFelipe and Jones, 1992; Résibois and Rogers, 1992). The distribution of cortical neurons containing these calcium-binding proteins has been shown to differ, in certain instances, from area to area in the primate cerebral cortex (Ferrer et al., 1992; Hof and Nimchinsky, 1992; Carmichael and Price, 1994; Condé et al., 1994; Kondo et al., 1994; Hof et al., 1995a). In particular, gradients of in the density of calbindin-immunoreactive neurons has been reported in the visual cortex of the macaque monkey, where the primary visual areas show much lower densities compared to visual association areas located in the parietal and temporal cortex (Kondo et al., 1994). Previous analyses of the distribution of calcium-binding proteins in the macaque monkey cingulate cortex have shown that parvalbumin-immunoreactive interneurons are codistributed with neurofilament protein-immunoreactive pyramidal cells along the ventro-dorsal and rostro-caudal axes of the cingulate cortex, whereas calbindin and calretinin immunostaining show a somewhat more monotonous laminar and regional patterns (Hof and Nimchinsky, 1992; Carmichael and Price, 1994). Comparably, the distribution of calcium-binding proteinsin the human orbitofrontal cortex demonstrates relatively homogeneous patterns for parvalbumin- and calretinin-immunoreactive interneurons, whereas parvalbumin immunoreactivity in the neuropil shows substantial variability among orbitofrontal cortex subareas including patterns compatible with the distibution of thalamocortical inputs (Hof et al., 1995a).

Thus, variations in the distribution of calcium-binding proteins might reflect differences in the intrinsic organization of various cortical areas that would have functional implications for regional specialization in cortical processing. Since these soluble cytoplasmic proteins are also present in projection neurons in thalamic nuclei (Hashikawa et al., 1991; Rausell and Jones, 1991a,b; Rausell et al., 1992a,b; Diamond et al., 1993; Blümcke et al., 1994; Jones et al., 1995; Molinari et al., 1995), the terminals of these neurons in the cortex also contain them, producing patterns of neuropil staining that vary with cortical areas and define thalamocortical terminal fields (Blümke et al., 1990, 1991, 1994; DeFelipe and Jones, 1991; Diamond et al., 1993; Carmichael and Price, 1994; Hof et al., 1995a; Molinari et al., 1995). In this context, preliminary evidence from our laboratory indicates that calretinin immunoreactivity patterns in the neuropil of the human cingulate cortex correlate well with the presence of calretinin in thalamic nuclei that are known to project to specific fields of the cingulate cortex in primates and indicate that calretinin may be a reliable tool for studying select neuronal systems in the human cerebral cortex (Vogt et al., 1993).

Such biochemical approaches to cytoarchitecture, or chemoarchitectonics, are powerful tools for the definition of cortical areas. The present study was designed to determine whether differences in cortical cytoarchitecture in the cingulate gyrus are accompanied by variations in

chemoarchitecture, and whether these differences respect the borders defined on Nissl-stained materials. If this were the case, these markers could facilitate the identification of cortical areas that might otherwise be very difficult to resolve. Furthermore, to the extent to which such markers can be linked to aspects of thalamocortical connectivity, staining patterns with these markers, combined with a knowledge of the connections in the nonhuman primate, could provide clues to the subcortical connectivity of these cortical areas in the human brain.

MATERIALS AND METHODS

Human brains were obtained at autopsy from seven patients with no history of neurologic or psychiatric disorders (five women, two men; 82.3 ± 9.5 years old, range: 70–96). Clinical data on the cases were available from the medical records of the Division of Neuropathology, Mount Sinai Medical Center, New York, the Department of Psychiatry, University of Geneva School of Medicine, Switzerland, and the Department of Anatomy, University of Navarra, Pamplona, Spain. The materials were collected according to appropriate ethical guidelines and all protocols were reviewed and approved by the relevant institutional committees. In all of the cases, neuropathological evaluation revealed scarce neurofibrillary tangles restricted to layer II of the entorhinal cortex. Neurofibrillary tangles were not observed within the cingulate cortex, and rare senile plaques or amyloid deposits were found in the hippocampal formation and neocortex. The post-mortem delay ranged from 1 to 10 hours. In one case, the brain was perfused shortly after death through the carotid arteries with 4% paraformaldehyde. A series was available from this brain of the medial portion of the hemisphere from the frontal pole through the entire cingulate gyrus. In all other cases, the brains were hemisected at autopsy, and one hemisphere was fixed whole in 4 liters of cold 4% paraformaldehyde overnight.

The entire cingulate gyrus was dissected out of the hemispheres and removed intact. The brain samples were placed into fresh 4% paraformaldehyde and post-fixed for up to 72 hours longer. The samples of the cingulate gyrus were then dissected either into 1 cm thick coronal blocks (in three cases) or parasagittally (in three cases), separating the medial face containing largely areas 24b and 23b from the rest of the gyrus. The blocks were then cryoprotected by immersion in solutions of increasing concentrations of sucrose, from 12 to 30% in phosphate-buffered saline (PBS). Blocks were frozen on dry ice and cut at 40 μm on a cryostat or sliding microtome. Two series were taken every 25 sections, with the result that the entire gyrus was sampled once every millimeter. After sectioning, the sections were rinsed thoroughly in PBS, treated in a solution of 0.75% hydrogen peroxide in 75% methanol for 20 minutes to eliminate endogenous peroxidase activity, rinsed again, and then placed into a solution of primary antibody in a diluent containing 0.3% Triton X-100 and 0.5 mg/ml bovine serum albumin. Four consecutive series of sections were incubated with antibodies that recognize, respectively, nonphosphorylated epitopes on the mid and heavy molecular weight subunits of the neurofilament protein triplet (SMI-32, Sternberger Monoclonals, Baltimore, MD; dilution, 1:5000; Sternberger and Sternberger, 1983; Lee et al., 1988), or the calcium-binding proteins parvalbumin, calretinin (Swant, Bellinxona, Switzerland; dilution, 1:3000; Celio et al., 1988, 1990) or calbindin (Swant; dilution, 1:1500; Schwaller et al., 1993). Tissue was incubated for a minimum of 40 hours on a rotating table at 4°C. Following incubation, sections were processed by the avidin-biotin method by using a Vectastain ABC kit (Vector Laboratories, Burlingame, CA) and intensified in 0.0067% osmium tetroxide. Another series was stained with cresyl violet to permit comparisons with the cytoarchitecture of these areas (Vogt et al., 1995).

Analyses were performed by using a computer-assisted morphometry system consisting of a Zeiss Axiophot photomicroscope equipped with a Zeiss MSP65 computer-controlled motorized stage (Zeiss, Oberkochen, Germany), a Zeiss ZVS-47E video camera system (Zeiss, Thornwood, NY), a Macintosh 840AV microcomputer, and custom designed morphometry software developed in collaboration with the Scripps Research Institute (La Jolla, CA; Young et al., 1996; Bloom et al., 1997). For the generation of unfolded cortical maps, every fourth section was mapped at low magnification. At the crests and fundi of all gyri and sulci, the border between layers III and V or the middle of layer IV was indicated as a landmark, and the distances between adjacent landmarks were measured. These measurements were plotted to make a flat rendering of the cingulate gyrus so that the cortex buried in the callosal and cingulate sulci was exposed. No attempt was made to flatten vertical sulci. Neurons were mapped by using NeuroZoom (Nimchinsky et al., 1996; Young et al., 1996; Bloom et al., 1997), and the length of the cortex divided into 100 μm wide bins. The mapped neurons in each bin were counted, and the frequency distribution plotted on the flattened map. Counts were not performed in a stereologic manner, since the intention was only to represent the distribution of these neurons in relative terms. The parcellation and terminology of the cingulate gyrus used was that of Vogt et al. (1995).

RESULTS

Distribution of neurofilament protein-immunoreactive neurons

Immunocytochemical staining with an antibody to a nonphosphorylated epitope on the neurofilament protein yielded a staining pattern which differs in the anteroposterior and ventrodorsal axes. The most obvious change observed was between the anterior cingulate cortex, where neurofilament protein-immunoreactive neurons were present only in layers V and VI, and posterior cingulate cortex, where neurofilament protein-immunoreactive neurons were found also in layer III (Fig. 1). This rostrocaudal change occurred gradually, with neurofilament protein-immunoreactive layer III neurons appearing, sporadically at first, in the most dorsal portions of the gyrus, and then increasing in density more ventrally, until layer III neurofilament protein-immunoreactive neurons were visible deep in the callosal sulcus.

In anterior areas 25 and 24, neurofilament protein-immunoreactive neurons were more scarce overall than in areas dorsal to the cingulate sulcus (Fig. 2). As shown in Figure 3A, most were in layer Va and some were in layers Vb and VI. A few lightly labeled neurons were in layer III, and intensely labeled stellate neurons appeared periodically in layer II. In layer VI, there was a large number of medium-to-light neurofilament protein-immunoreactive neurons whose sizes ranged from small to medium and whose shapes ranged from truly pyramidal to multipolar,

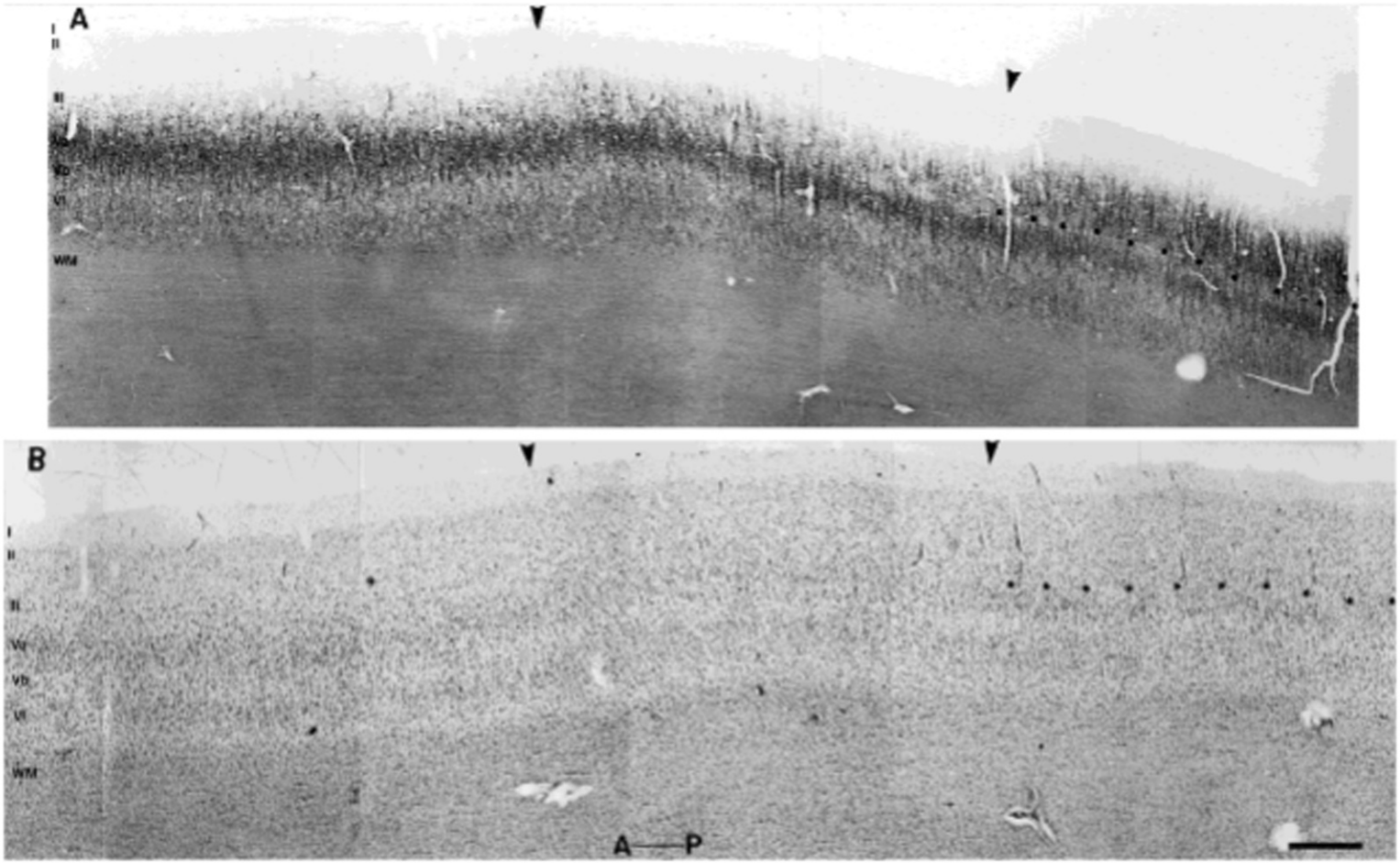

Fig. 1. Distribution of nonphosphorylated neurofilament protein-containing neurons in a horizontal section through the human cingulate gyrus **(A)** compared to a nearly adjacent Nissl-stained section **(B)**. This section occupies the middle portion of the gyrus, and includes the transition between areas 24 and 23 (posterior arrowhead). Note that at this level on the medial wall of the hemisphere, neurofilament protein-containing neurons appear in layer III rostrally to the border between areas 24 and 23 (anterior arrowhead). Layers are indicated by Roman numerals. Note the prominent layer Va and the presence of a layer IV in area 23 only (stars). A—P, Anterior-posterior axis. WM, white matter. Scale bar = 1 mm.

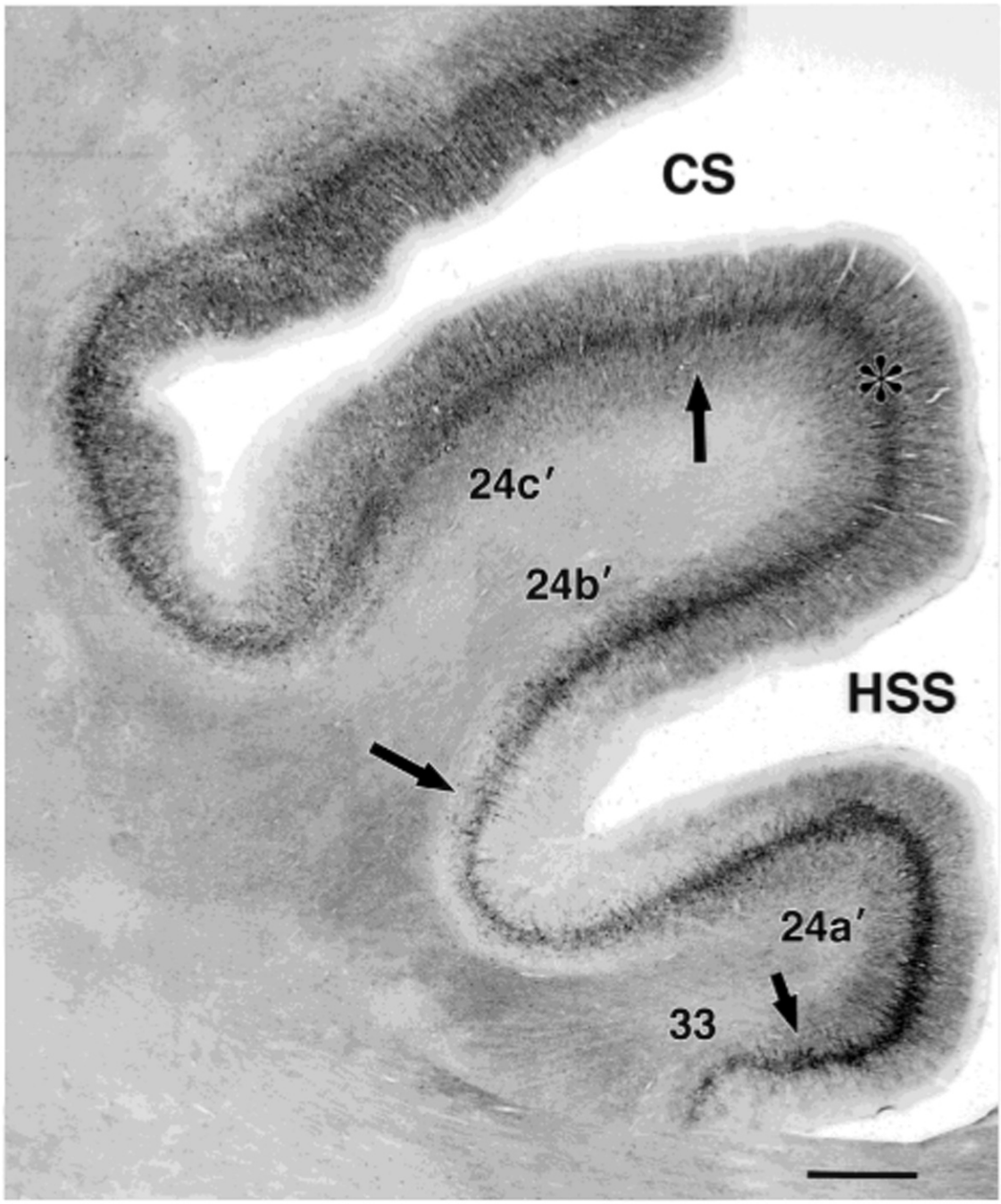

Fig. 2. Distribution of nonphosphorylated neurofilament protein-containing neurons in a coronal section through the human anterior cingulate cortex. Note the near absence of neurofilament protein-containing neurons in layer III in the ventral portion of the gyrus, and the increase dorsally. Areal borders are indicated by arrows; layer Va is indicated by an asterisk. This figure was prepared electronically by scanning the photographic negative on a high resolution flatbed transilluminating scanner (Microtek, Redondo Beach, CA). The digitized image was imported, composited, and labeled with Adobe Photoshop software (version 3.0.1, Adobe Systems, Mountain View, CA). The resulting digital file was then printed on a Fujix Pictography 3000 system (Fuji Photo Film, Elmsford, NY). Only minor contrast adjustments were made for optimal printing quality, which did not alter the appearance of the original data (Vogt et al., 1995). CS, Cingulate sulcus; HSS, horizontal secondary sulcus. Scale bar = 1 mm.

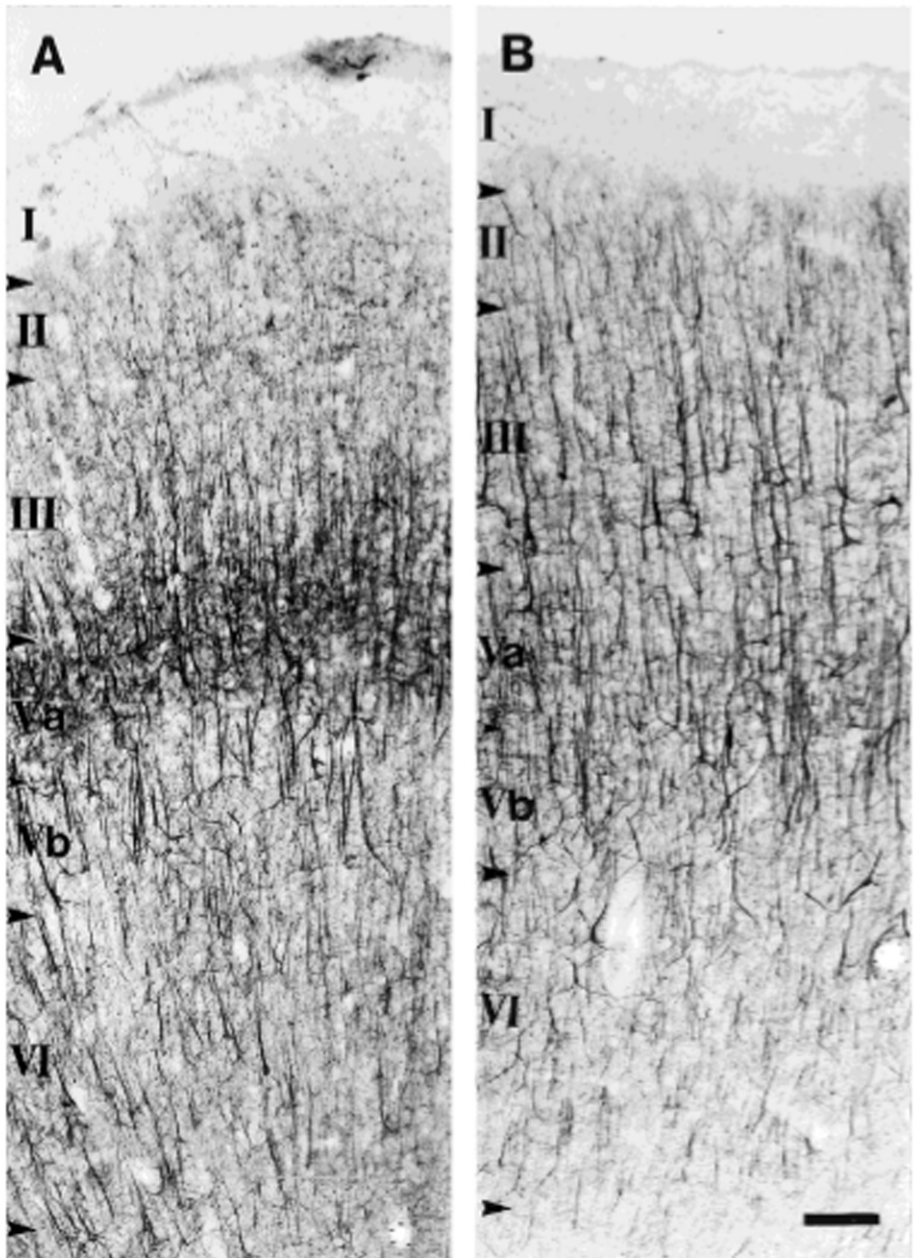

Fig. 3. Distribution of nonphosphorylated neurofilament protein-containing neurons in areas 24a **(A)** and 24c' **(B)** of the human cingulate cortex. Area 24a is marked by the virtual absence of neurofilament protein-immunoreactive neurons in superficial layers, and a compact layer Va densely populated with immunoreactive neurons and their proximal dendrites. Layer Vb is markedly sparser, and contains numerous immunoreactive spindle neurons. Area 24c', in contrast, contains a substantial population of immunoreactive neurons in layer III, and has a sparser layer Va. Scale bar = 150 μm.

horizontal or fusiform. The most prominent population was found in layer Va, where clusters of immunoreactive typical pyramids were found. Layer Vb was sparser, and contained numerous immunoreactive spindle neurons (Nimchinsky et al., 1995). In the most anterior portions of area 24, this pattern was the same for all the subdivisions

of area 24. More caudally, immunoreactive neurons appeared in layer III, first in the most dorsolateral portions of the gyrus, then progressively more ventrally and medially. Area 24′ between areas 24 and 23 was characterized by an increasing frequency of layer III neurofilament protein-immunoreactive pyramidal neurons (Fig. 3B). However, the area marked anteriorly by the appearance of the first of these neurons and posteriorly by a densely populated layer III was much larger than that occupied by the transition zone between anterior and posterior cingulate cortex as defined by Nissl stain. Thus, area 24a′ contained very few immunoreactive layer III neurons, subarea 24b′ contained a few, and subarea 24c′ contained a considerable number.

In area 23, all three subdivisions contained immunoreactive neurons in layer III. These neurons were more prominent in areas 23a and 23c than in 23b. In area 23a, the immunoreactive pyramidal neurons formed clusters and were distributed throughout the thickness of layer III (Fig. 4B). In contrast, in areas 23b and 23c, the layer III pyramidal neurons were arranged in rows, and tended to be located in the deepest portion of layer III (Fig. 4C). In the caudal portion of the callosal sulcus, area 29 contained two layers with immunoreactive neurons: layers III and V (Fig. 4A). Area 30 had progressively more immunoreactive neurons in layer III in the lateromedial direction and an increase in the number of immunoreactive neurons in layer VI. Relative to area 23a, there were few immunoreactive neurons in layer V.

Distribution of calcium-binding protein immunoreactivity

Immunoreactivity for calcium-binding proteins gave rise to two distinct types of labeling: neurons and neuropil. They will be described separately in the following paragraphs. In general, immunoreactive neurons had distributions that respected cytoarchitectural boundaries to some degree, while most neuropil labeling patterns changed more gradually along the gyrus, resulting in the trends described below.

Parvalbumin. Immunoreactive neurons. In the most anterior portions of area 24, parvalbumin immunoreactivity for both neurons and neuropil was much more intense dorsally than ventrally (Fig. 5). In most of area 24, parvalbumin-immunoreactive neurons were found principally in layer V. In anterior area 24a, however, virtually none were found, even in layer V (Fig. 6A), as was the case in areas 25 and 33. More caudally in area 24a and in area 24b, more layer V neurons appeared, and still more were found in area 24c (Fig. 6B,C). These neurons were frequently clustered, giving the neuropil labeling of layer V a patchy, discontinuous quality (Fig. 6B,C). Parvalbumin-immunoreactive layer III neurons began to appear in area 24a, but these were very sparse. More were apparent in area 24c (Fig. 6C). In addition, parvalbumin-immunoreactive layer II neurons appeared in area 24c (Fig. 6C). In area 24b, there was a zone between the layer III and layer V parvalbumin-immunoreactive neurons that was virtually devoid of immunoreactivity. This zone did not appear in the lateral portion of area 24c, where immunoreactive neuronal somata were found throughout layers II–VI. Vertically oriented parvalbumin-immunoreactive cartridges, possibly representing the terminals of chandelier neurons on the initial segments of layer V pyramidal cell axons (DeFelipe et al., 1989; Lewis and Lund, 1990; Williams et al., 1992; Kalus and Senitz, 1996) were abundant in layers V and VI in the anterior cingulate cortex, in all of its subdivisions (Figs. 6C, 8D), while far fewer were found in layers II and III. In areas 24a′ and 33, layer II was characterized by a population of occasionally large immunoreactive somata (Fig. 7A). In addition, in areas 33 and 24a′, labeled neurons were very scarce in the deep portion of layer VI, whereas in areas 24b′ and 24c′, clustered immunoreactive neurons were frequently encountered in this layer. These patterns continued into area 23, where, as described above, layer IV contained parvalbumin-immunoreactive neurons (Fig. 8A,B).

Neuropil labeling patterns. In area 25, there was very light neuropil labeling (Fig. 6A). Most of the labeling appeared to be due to the presence of axons and dendrites of immunoreactive neurons in layer V. Increased neuropil labeling was observed in layers III and V of area 24a (Fig. 6B). In areas 24b and 24c, a band of parvalbumin-immunoreactive neuropil appeared in the deep portion of layer III, and it was more intense dorsally, such that in area 24c, it was very intense (Fig. 6C). This band coincided with the presence of immunoreactive layer III neurons, but it was also evident ventrally, where immunoreactive neurons were very rare. More caudally within area 24, in area 24′, this immunoreactive band appeared more ventrally, until it reached area 24a′, and even area 33 in the depth of the callosal sulcus (Fig. 7A). In area 33, the caudal portion of areas 24a′ and 23a, the neuropil was labeled from layer I through layer V (Fig. 8A), in contrast to the pattern more rostrally, where the neuropil immunoreactivity was restricted to layers III and Vb (Fig. 7A,B). In particular, layer II was characterized by very dense neuropil labeling, from which fibers extended into layer I (Fig. 8A). In one case, the pattern of immunoreactivity in area 24a′ extended onto the gyral surface, stopping at the dimple parallel to the cingulate sulcus, which delineated the border between area 24a′ and 24b′, as described by Vogt et al. (1995). In area 24′, the emphasis of the neuropil labeling shifted gradually from dorsal to more ventral regions. These patterns continued into area 23, where the deep portion of layer III and layer IV was occupied by dense parvalbumin-immunoreactive neuropil labeling (Fig. 8B). In areas 29 and 30, layer IV contained immunoreactive neurons, but there was no obvious neuropil labeling to demarcate these areas from area 23 (Fig. 8C). The variations in parvalbumin-immunoreactive neuropil labeling are summarized schematically in Figure 9. On a cytoarchitectonic flattened map of the cingulate cortex (Fig. 9A), the patterns of neuropil labeling with parvalbumin can be seen to vary in a manner largely irrespective of sulcal and cytoarchitectonic boundaries (Fig. 9B,C).

Calbindin. Immunoreactive neurons. In area 25, calbindin-immunoreactive neurons were mostly in superficial cortical layers (Fig. 10A). Intensely immunoreactive nonpyramidal neurons were concentrated in layer II and the superficial portion of layer III. Their somata were generally round-to-ovoid, and were comparable in size to those immunoreactive for calretinin. In layer VI, a separate population of neurons was present, and these tended to be multipolar and somewhat less intensely immunoreactive. Lightly immunoreactive pyramidal neurons were visible in layers II and III. In area 24, immunoreactive neurons appeared in layer III and, to a lesser extent, layers V and VI (Fig. 10B,C). The cellular patterns were comparable among areas 24a, 24b, and 24c. However, in ventral area 24a, there were very few immunoreactive neurons in the labeled neuropil of the deep portion of layer III (Fig. 10B).

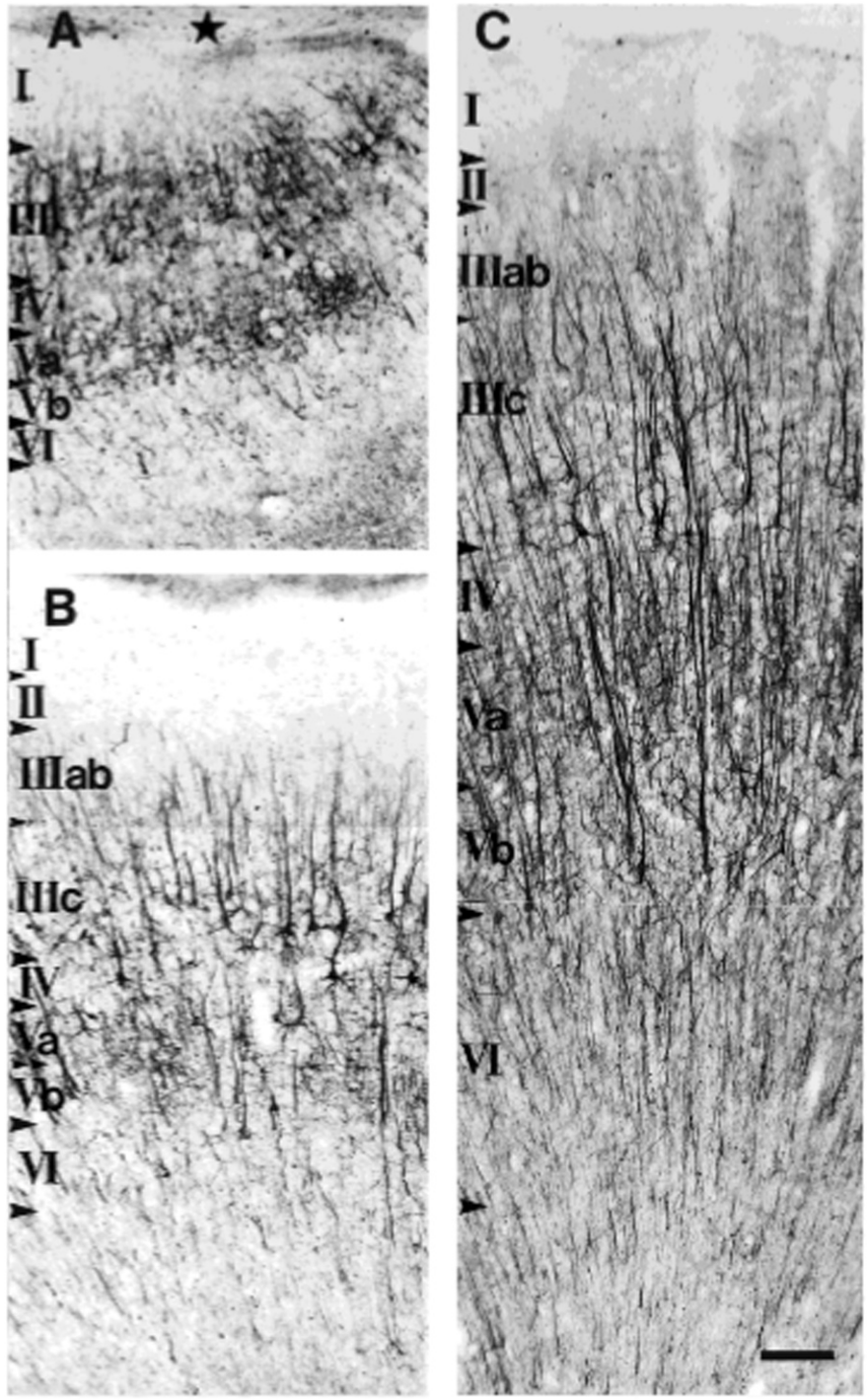

Fig. 4. Distribution of neurofilament protein-containing neurons in the lateral aspect of area 29 (**A**), and areas 23a (**B**) and 23b (**C**) of the human cingulate cortex. In area 29, two major layers are clearly discernable, III and Va. Layer II is not present in area 29l, but it is in the adjacent area 30. Layer III contains scattered large neurons, which frequently appear also in layer IV. Layers Vb and VI are neuron-sparse. The star indicates the corpus callosum. Areas 23a and 23b both contain a well-defined layer IV on Nissl-stained materials, which is represented here as an immunoreactive soma-sparse zone between layers IIIc and V. In area 23a, the large pyramidal neurons in layer IIIc are scattered throughout the thickness of the layer, whereas in area 23b, the layer IIIc neurons are more restricted to the deepest portion of the layer. Note the immunoreactive apical dendrites of layer V neurons that can be seen ascending through layer IV in area 23b. Scale bar = 150 μm.

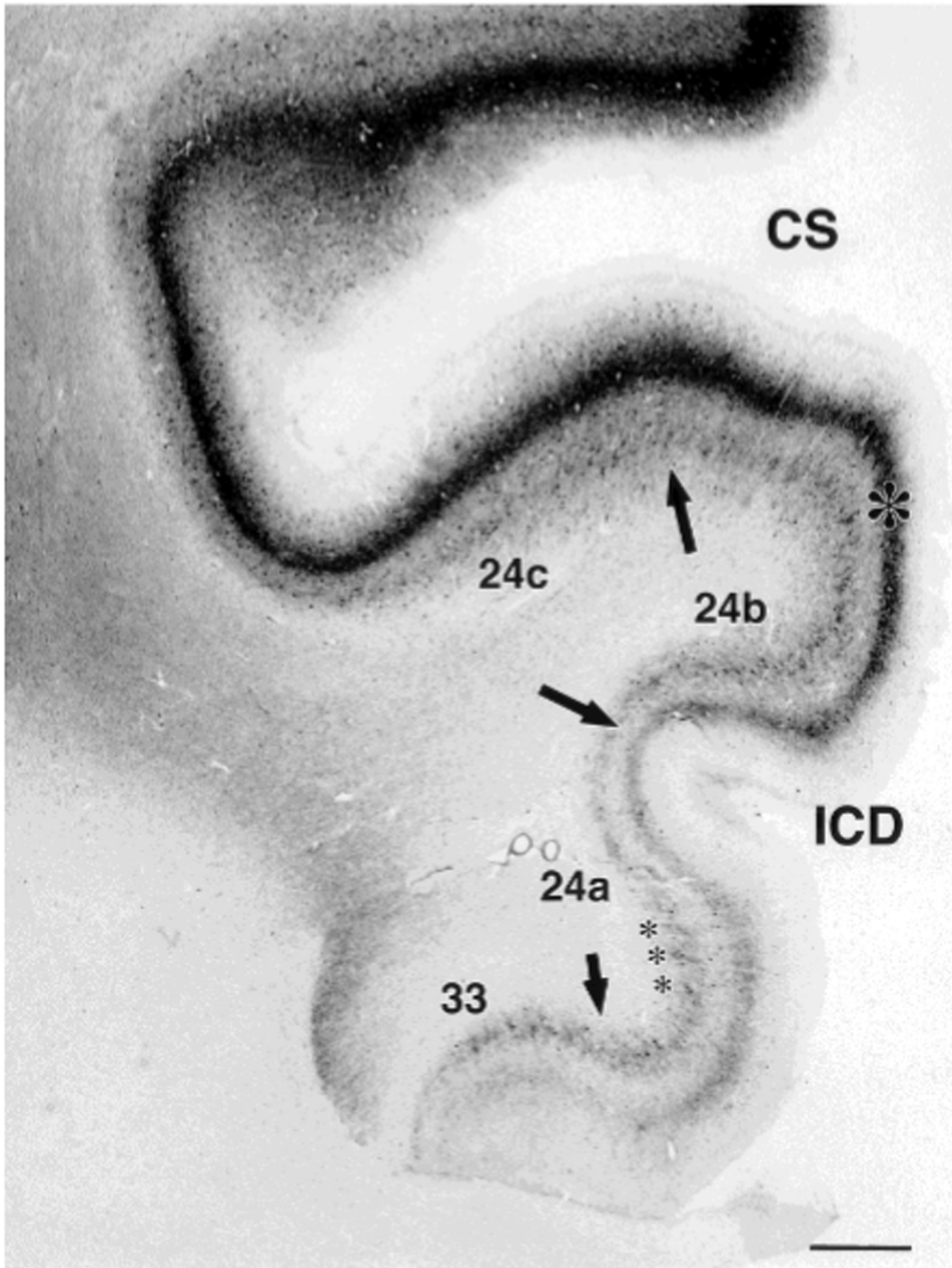

Fig. 5. Distribution of parvalbumin immunoreactivity in a coronal section through the human anterior cingulate cortex. Note the intensity of immunoreactivity in dorsal portions of the gyrus, and the extreme reduction of immunoreactivity ventrally. Layer III is indicated by the large asterisk. Patches of immunoreactive neuropil in layer Vb are evident even at this low magnification (small asterisks). Areal borders are indicated by arrows. See Figure 2 legend for details on photographic processing. ICD, Intracingulate dimple; CS, cingulate sulcus. Scale bar = 1 mm.

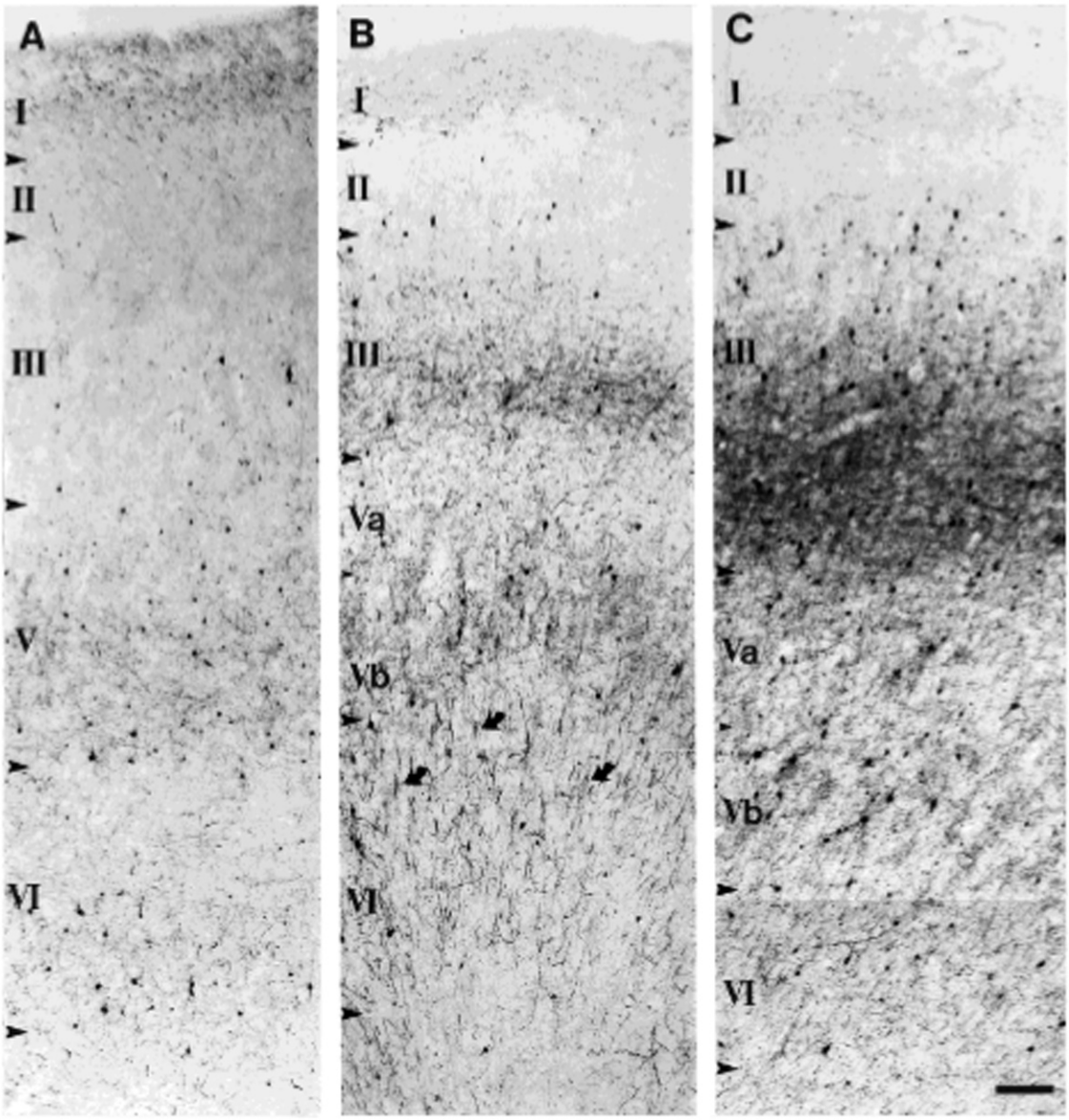

Fig. 6. Distribution of parvalbumin immunoreactivity in areas 25 **(A)**, 24a **(B)**, and 24c **(C)** in the human cingulate cortex. Area 25 contains the fewest immunoreactive neurons and the lightest neuropil staining in the cingulate cortex. Most immunoreactive neurons are found in layers V and VI, and most of the immunoreactive fibers are localized to layer V. Area 24a contains immunoreactive neurons from layers II through VI, but most are concentrated in layers III and Vb. Layer III is characterized by a band of neuropil staining in its deepest portion, and layer Vb contains patches of immunoreactive labeling. Layer Va is relatively lightly stained. Immunoreactive presumptive cartridges of chandelier neurons are most abundant in layer VI (curved arrows), and are shown at higher magnification in Figure 8D. Area 24c contains a very intensely immunoreactive band of neuropil labeling that extends throughout the deeper half of layer III. Immunoreactive clusters in layer Vb are also evident in this area, and cartridges are reduced in number. Scale bar = 150 μm.

A few appeared in area 24b, but area 24c was characterized by a considerable number of nonpyramidal neurons in this sublayer (Fig. 10C). Area 33 contained very few immunoreactive nonpyramidal neurons, and virtually no immunoreactive pyramidal neurons. In area 24′, immunoreactive pyramidal neurons were somewhat reduced in comparison with area 24 (Fig. 11A,B). With the appearance of layer IV in area 23, this layer became populated

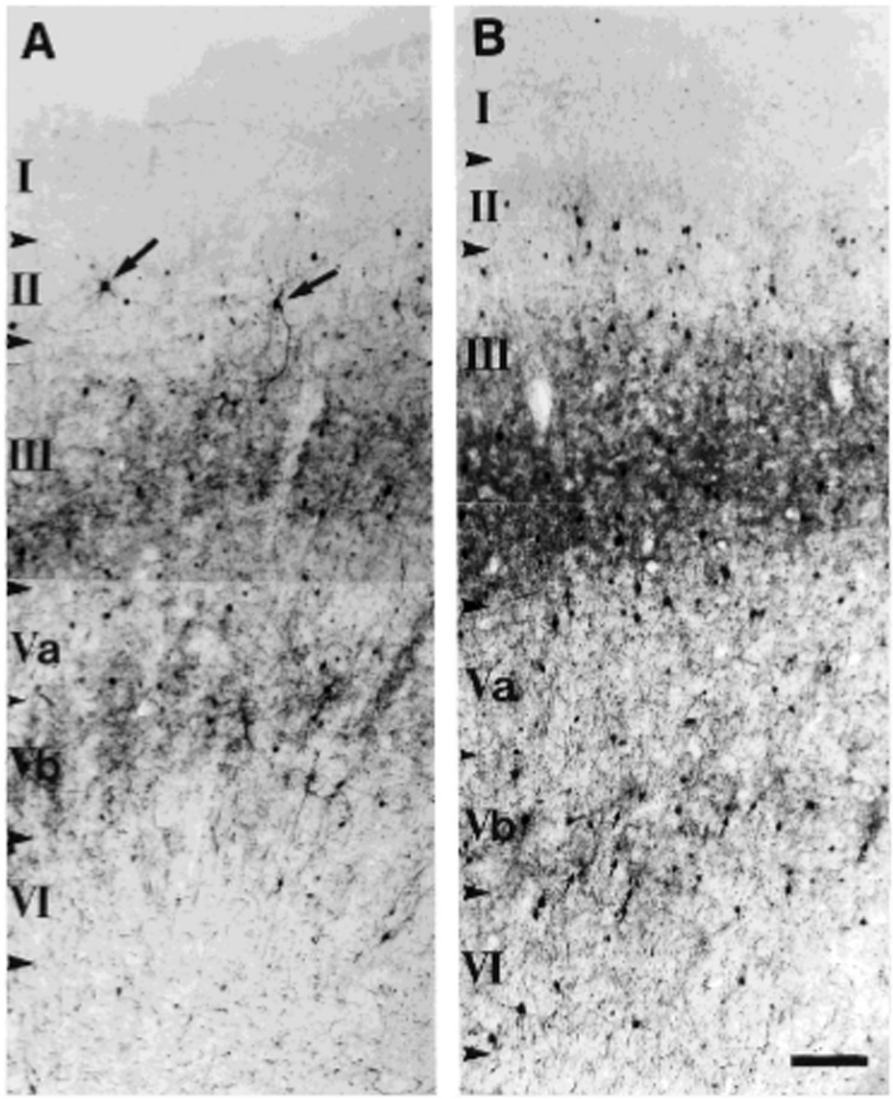

Fig. 7. Distribution of parvalbumin immunoreactivity in areas 24a′ (**A**) and 24c′ (**B**) in the human cingulate cortex. Note the presence of large parvalbumin-conatining neurons (arrows in A) and the increase in immunoreactive neuropil labeling in layer III of area 24a′ compared with that found in area 24a (Fig. 6B). Area 24c′ has a well-defined layer Va showing a lower labeling intensity than area 24c (Fig. 6C), and small patches (small arrows) of immunoreactive labeling in layer Vb. Scale bar = 150 μm.

with immunoreactive neurons (Fig. 12A–C). Area 23 contained the fewest calbindin-immunoreactive pyramidal neurons in the cingulate gyrus (Fig. 12B).

Neuropil labeling patterns. Area 25 was characterized by the lightest neuropil staining in the cingulate gyrus (Fig. 10A). In area 24, the neuropil was stained from layer II through the deep portion of layer III. This labeling was incremental, with layer II lightest and the labeling increasing in intensity with the cortical depth (Fig. 10B,C). Layers I, V, and VI were largely unstained, except for immunoreactive patches in layer V. The neuropil staining was not homogeneous. Intensely labeled beaded fibers were visible in the deep layers, and could often be attributed to immunoreactive nonpyramidal neurons. The intensity of the staining in the neuropil increased from area 24a through area 24c, and what appeared in area 24a as an increasing superficial-to-deep gradient of neuropil immunoreactivity became resolved in area 24c as an immunoreactive band in layer III (Fig. 10C). The neuropil in area 33 was also very lightly labeled. In area 24′, the patches of

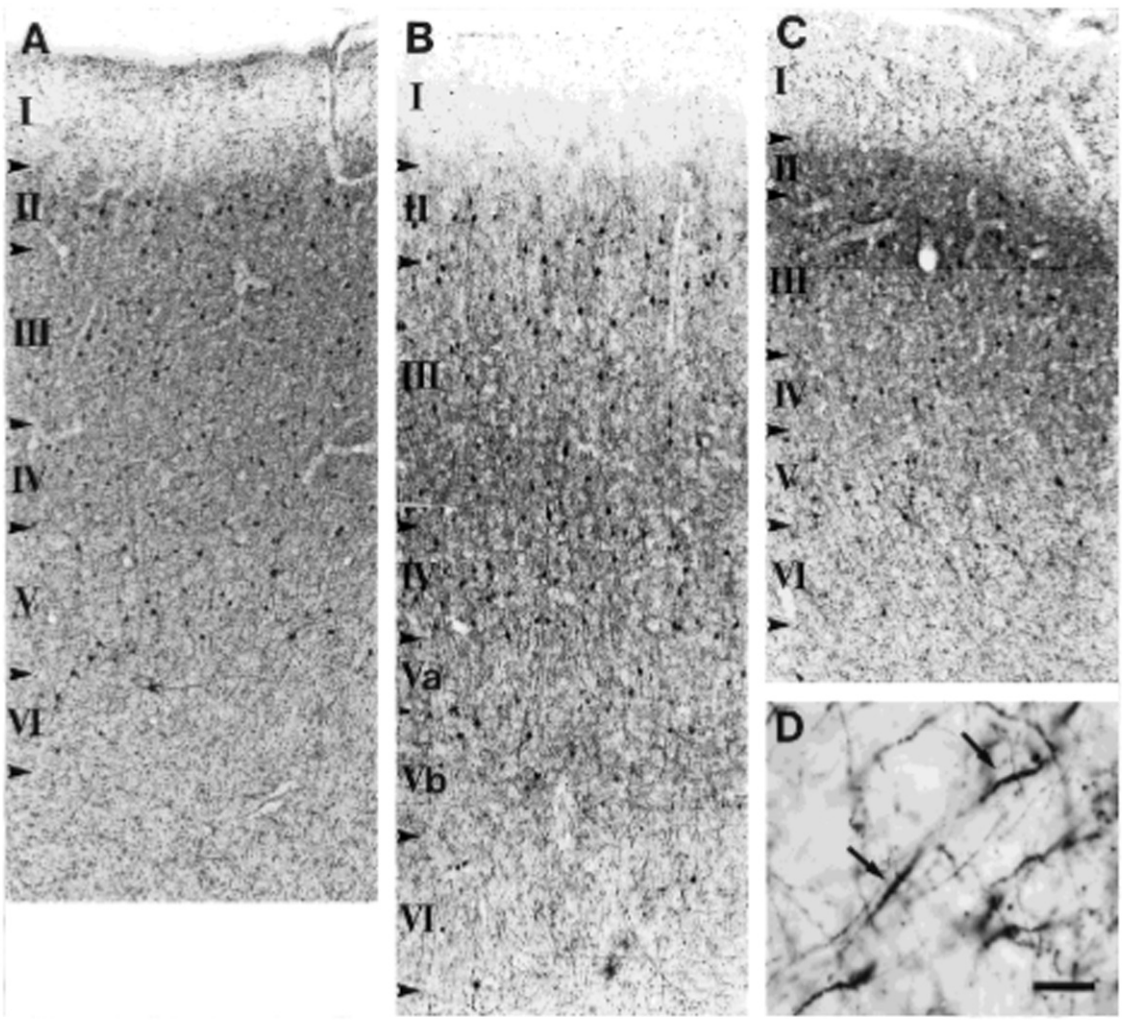

Fig. 8. Distribution of parvalbumin immunoreactivity in areas 23a (**A**), 23b (**B**), and 29 (**C**) in the human cingulate cortex. Area 23a, and parts of area 23b more caudally, area characterized by moderate-to-intense, fairly homogeneous neuropil labeling in layers II through VI. No distinct band is visible (A). In contrast, much of area 23b, and all of area 23c contains an intensification in neuropil labeling in the deep portion of layer III and in layer IV (B). Area 29 (C) resembles area 23a, but is significantly thinner. Parvalbumin-immunoreactive presumptive cartridges (arrows) of chandelier neurons in layer VI of area 24a' are shown in (**D**). These structures were most abundant in layer VI (Fig. 6B), and varied in length from less than 20 μm to over 50 μm. Scale bar = 150 μm in A–C and 25 μm (D).

immunoreactive fibers in layer V became more pronounced, especially in area 24a' (Fig. 11A). The neuropil in layers V and VI became labeled, leaving only layer I unstained (Fig. 11B). Within area 24', the band of immunoreactive neuropil gradually extended ventrally until it reached the depth of the callosal sulcus, thus labeling areas 33 and 24a'. In area 23a, the band of neuropil occupied layers II through V (Fig. 12A), and was thus reminiscent of the pattern observed with parvalbumin (Fig. 8A). Area 23c contained an immunoreactive band only in layers II and III, not throughout its thickness (Fig. 12B). In areas 29 and 30, the staining pattern resembled that in area 23a. No distinctive neuropil staining was observed in these areas (Fig. 12C).

Calretinin. Immunoreactive neurons. In the anterior cingulate cortex, as described elsewhere in the primate neocortex, intensely immunoreactive calretinin-containing neurons were found mostly in layer II and the superficial portion of layer III (Hof et al., 1993b; Condé et al., 1994). These were nonpyramidal neurons, whose morphology resembled that of bitufted neurons. Occasionally, immunoreactive neurons resembled bipolar neurons. Their somata were ovoid-to-fusiform, and their dendrites, frequently beaded, could often be seen coursing radially

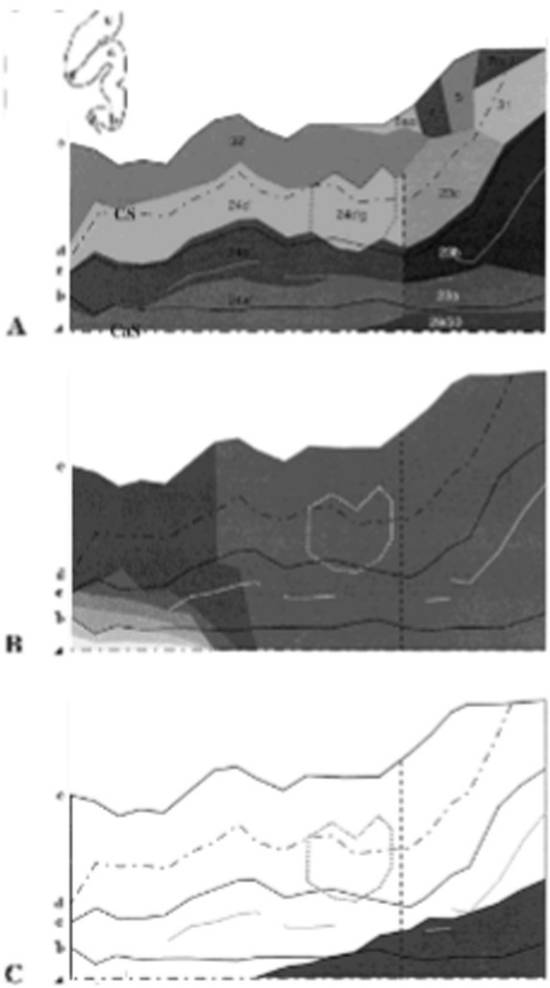

Fig. 9. Flattened representation of the cingulate cortex in a human brain, showing the localization of subareas based on Nissl stain according to Vogt et al., 1995 (**A**; regions are shown by different gray tones), and changes in parvalbumin-immunoreactive neuropil labeling observed along the gyrus (**B, C**). Only the part of the cingulate cortex dorsal to the body of the corpus callosum is shown in (A). The giguntopyramidal field (area 24c'g) is outlined with dotted lines, and a vertical broken line indicates the border between areas 24 and 23 as determined using the Nissl stain. The depth of the callosal (CaS) and cingulate (CS) sulci is indicated by dashed lines. The gyri crowns are shown by continuous lines. In (B) and (C), the gray scale indicates relative intensity of neuropil staining, and is not quantitative. Note the presence of two gradients: First, one of increasing intensity of immunoreactivity in layer III of the dorsal and posterior direction anteriorly in the gyrus (B); second, a pattern indicated by the dark outline in (C), representing the labeling gradient in cortical layers II through VI observed in areas 23a and parts of 23b (Fig. 8A). The dark region in the lower right corner of the map represents the gradual shift in neuropil labeling starting in area 24', and continuing into area 23, where the deep portion of layers III and IV was occupied by dense parvalbumin-immunoreactive neuropil labeling. The position of the sulcal and gyral landmark lines on the flattened map (**a–e**) is indicated in the inset.

through the cortex. Calretinin-immunoreactive neurons were occasionally encountered in layer I, and were presumed to represent Cajal-Retzius cells (Vogt Weisenhorn et al., 1994; Fonseca et al., 1995). Scattered immunoreactive neurons could be seen in the deep portions of layer III and layers V–VI. In layer VI, calretinin-immunoreactive neurons assumed numerous morphologies, including multipolar and horizontal forms. In addition, both areas 25 and 24 contained a unique population of calretinin-immunoreactive pyramidal-like neurons in layer V (Figs. 13A,B, 15). This population was most numerous in area 25, and in anterior and ventral portions of area 24. These neurons were more lightly labeled than the nonpyramidal neurons, and only their somata and most proximal dendritic arborizations were visible (Fig. 13C).

One significant difference in the laminar patterns of immunolabeled neurons between areas 24 and 24' confirmed this cytoarchitectural distinction. This was the presence of calretinin-immunoreactive layer V pyramidal-like neurons in area 24 (Fig. 14A). These neurons were present in large clusters in layer V, and their density dropped markedly in area 24'. In addition, there was another, sparser, population of calretinin-immunoreactive pyramidal-like neurons in area 24c'g (Fig. 13D). In the posterior portion of the gyrus, a few immunoreactive pyramidal-like neurons were found in layers V and VI in areas 29 and 30. Area 23 contained essentially no calretinin-immunoreactive pyramidal-like neurons (Fig. 14C). The density distribution of calretinin-immunoreactive pyramidal-like neurons is represented in Figure 15. Scattered calretinin-immunoreactive pyramidal-like neurons were also found through much of the anterior cingulate cortex up to the border with area 23, but their distributions were too sparse to appear on the flattened figure, since 100 μm-wide bins containing fewer than 10 such neurons were discounted (Fig. 15A). Area 25 also contained large numbers of these neurons (Fig. 15B), and these neurons occupied dorsal positions more caudally in the gyrus (Fig. 15C,D). With the appearance, in area 23, of layer IV, calretinin-immunoreactive nonpyramidal neurons were found in layer IV (Fig. 14C), but they were not as numerous as those labeled in this layer with parvalbumin.

Neuropil labeling patterns. Layer V of area 24 contained a meshwork of immunoreactive neuropil which lent a multilaminar appearance to the cortex. This meshwork was very dense, and appeared to be associated with the presence of calretinin-immunoreactive pyramidal neurons. With the disappearance of these neurons, the immunoreactive band of neuropil in layer V became less intensely labeled (Fig. 14A,B). In areas 29 and 30, there was an intensification of the neuropil labeling in layer IV (Fig. 14D). In cross-section, the immunoreactive band in layer V was patchy, and could be seen to shift from a more lateral position rostrally to a more medial position caudally.

DISCUSSION

Comparison with the Nissl stain

The present study demonstrates that the human cingulate cortex is, indeed, a region of considerable neurochemical heterogeneity. This variation along the gyrus is evident in the immunoreactivity of neuropil and of select neuronal populations, and the observed patterns were very consistent among the cases analyzed. In contrast with the areal borders described in Nissl-stained materials (Vogt et al.,

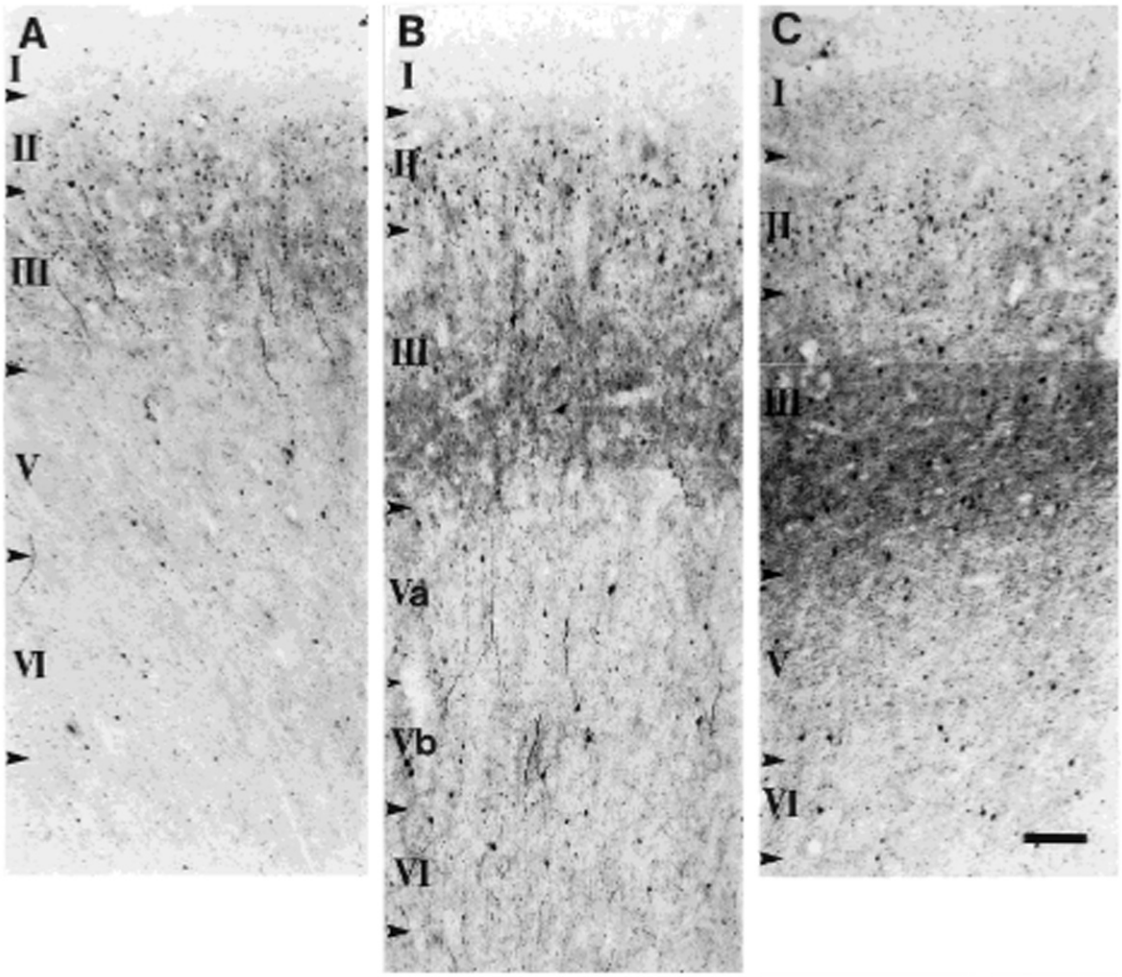

Fig. 10. Distribution of calbindin immunoreactivity in areas 25 (**A**), 24a (**B**), and 24c (**C**) of the human cingulate gyrus. In area 25, calbindin immunoreactivity is mostly neuronal, and largely consists of immunoreactive nonpyramidal and pyramidal neurons in layer II and the superficial portion of layer III (A). Area 24a is characterized by the addition of a band of immunoreactive neuropil in the deep portion of layer III, which is more compact and intense dorsally in area 24c. These neuropil labeling patterns are similar to those observed with parvalbumin (Fig. 6B,C). Scale bar = 150 μm.

1995, 1997), the boundaries defined by different distributions of neurofilament or calcium-binding proteins do not, as a rule, correspond to the parcellation of the cingulate cortex discretely into areas 24a–24c and 23a–23c. This is especially true of the neuropil labeling patterns, which vary in the dorsoventral axis irrespective of cytoarchitectonic boundaries, and in the anteroposterior axis show gradients rather than blocklike areal patterns. Even cellular markers have distributions that taper along the gyrus, rather than showing abrupt changes. However, neurochemically defined cell populations can have distributions that correlate with cytoarchitectonic boundaries. For instance, neurofilament protein-immunoreactive layer III neurons are notably absent in areas 25 and 24, but are present in areas 24′ and 23. Spindle neurons are virtually restricted to areas 25, 24, and 24′, and calretinin-immunoreactive pyramidal neurons are largely restricted to area 25 and 24, and areas 24a′ and 24b′. Thus, cell distributions, whether based on the Nissl stain or neurochemical markers, may yield parcellations that are to some extent comparable, whereas neuropil labeling, which reflects in part afferent systems and not cellular architecture, may provide other information about the connections of these areas. In this respect, the human cingulate cortex is characterized by neurochemical differences that reflect those found in the macaque monkey (Hof and Nimchinsky, 1992; Hof et al., 1993a; Vogt et al., 1993; Gabbott and Bacon, 1996b). There are certain cellular features, however, that distinguish the human from the nonhuman primate.

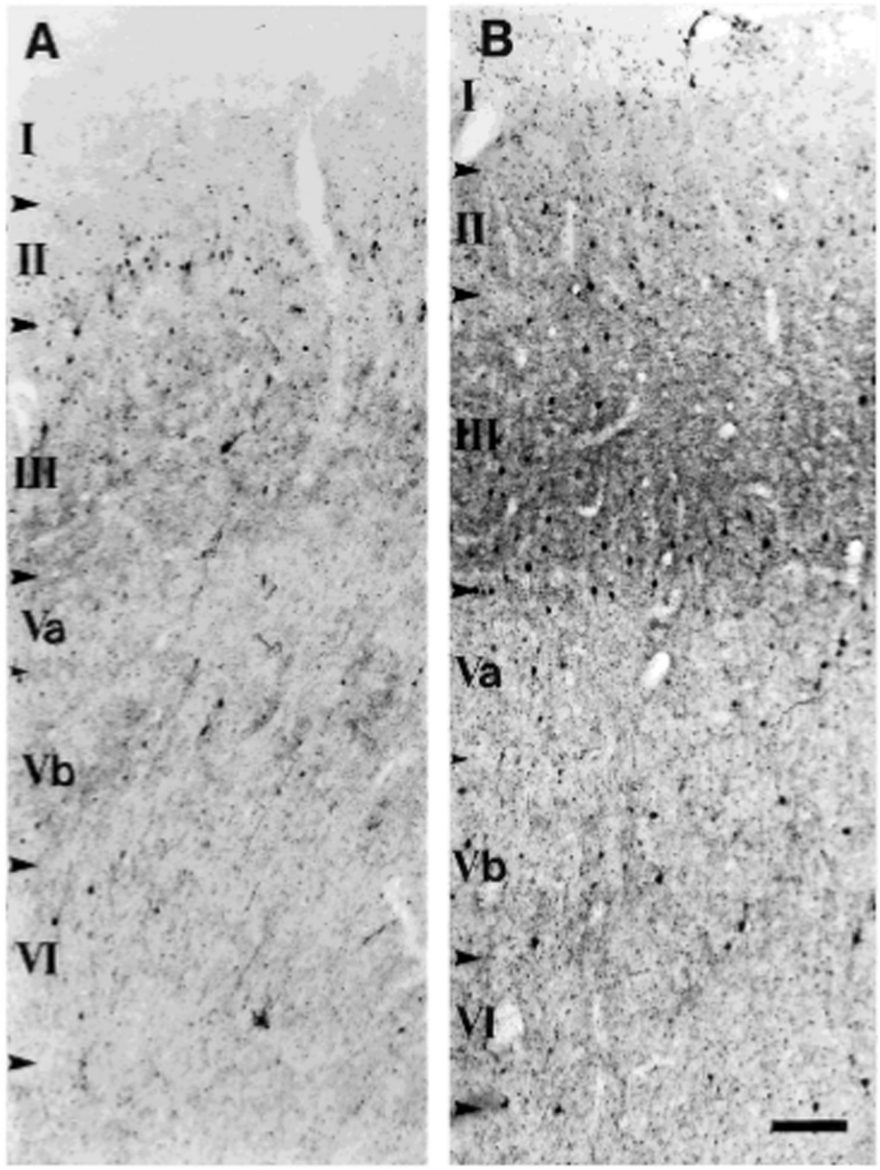

Fig. 11. Distribution of calbindin immunoreactivity in areas 24a′ (A) and 24c′ (B) of the human cingulate gyrus. Note the marked increase in neuropil labeling in layer III in the dorsal portion of the gyrus (B) compared to the ventral area (A). Some patchy neuropil labeling, similar to that observed with parvalbumin (Figs. 6B,C, 7A,B) is observed in layer Vb in area 24a′, but is not evident in area 24c′. Scale bar = 150 μm.

Neurofilament protein-immunoreactive neuron distribution varies along both the human and macaque monkey cingulate cortex

The changes described along the anteroposterior axis in the expression of neurofilament protein are globally comparable in the two species. Anteriorly, neurofilament protein-containing neurons are largely in deep layers and posteriorly, they are also in layer III. As in the monkey, the transition from the pattern found most anterior to that which characterizes the posterior cingulate cortex occupies a significant portion of the gyrus in the rostrocaudal axis (Hof and Nimchinsky, 1992). However, in the human,

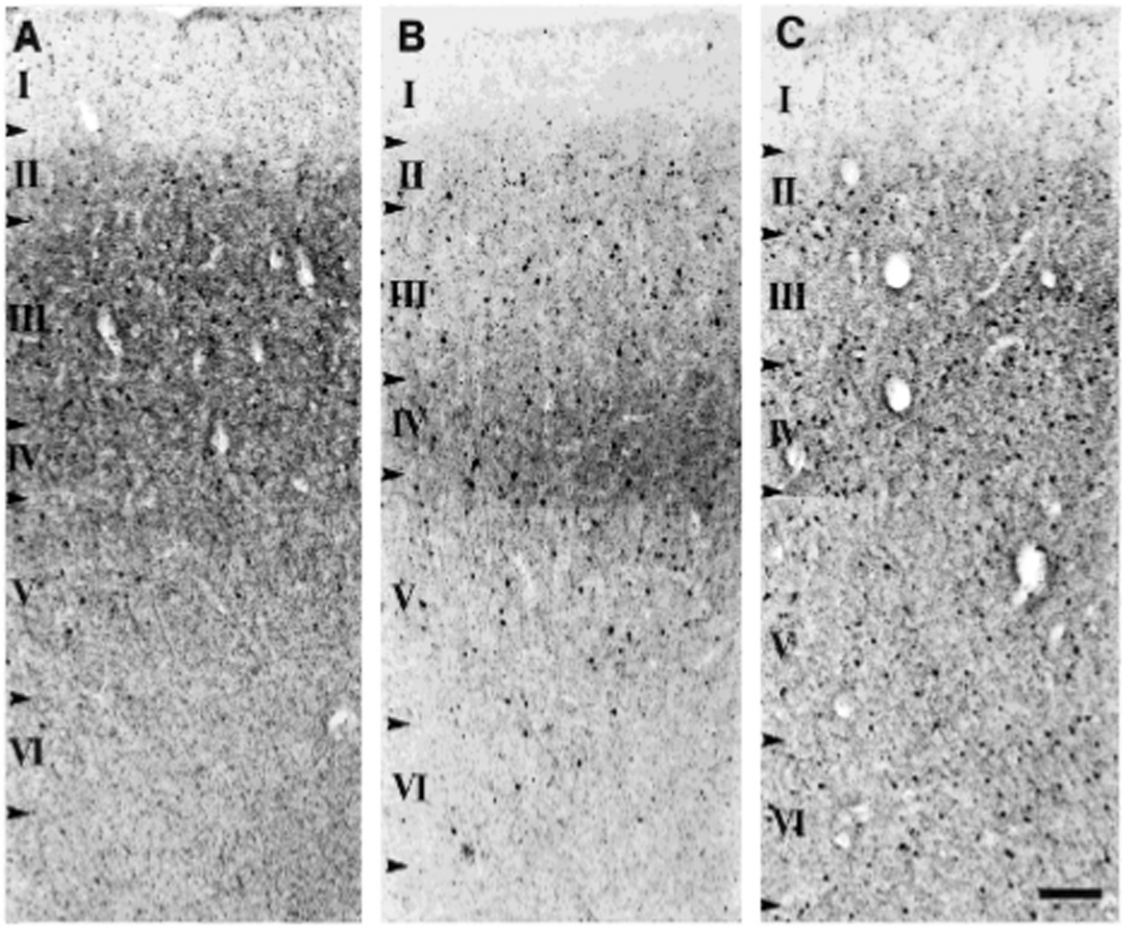

Fig. 12. Distribution of calbindin immunoreactivity in areas 23a (**A**), 23c (**B**), and 29 (**C**) of the human cingulate gyrus. Area 23a is characterized by neuropil labeling throughout layers II through VI, but mostly in layers II through V. In contrast, in area 23c, neuropil labeling is most intense in layer IV, and much weaker elsewhere. In both these areas, immunoreactive neurons are found in layers II through V, and to a lesser extent in layer VI. In area 29, a slight increase in the density of immunoreactive neurons is observed in layer IV, but no increase in neuropil labeling intensity is seen in areas 29 and 30. Scale bar = 150 μm.

layer III neurofilament protein-immunoreactive neurons appear relatively more rostrally in the dorsal portions of the gyrus, so that area 24b contains these neurons, whereas in the monkey it does not. Other differences include the presence, in the human, of immunoreactive spindle neurons in layer Vb of the anterior cingulate areas 24 and 24′ (Nimchinsky et al., 1995), and a distinct population of multipolar neurons in layer II. In addition, in the human, the population of neurofilament protein-containing neurons is much denser than in the monkey, although the overall staining pattern in the cingulate cortex is remarkably consistent in the two species.

Calcium-binding proteins label characteristic cellular features of the macaque monkey and human cingulate cortex

Parvalbumin-immunoreactive neurons manifest a pattern of distribution comparable to that observed in the nonhuman primate (Hof and Nimchinsky, 1992). Specifically, parvalbumin-immunoreactive neurons in the human cingulate cortex, as in the monkey, correlate with the presence of neurofilament protein-containing neurons on a regional basis. On the laminar level, however, this is not strictly true, since layer II frequently contains substantial numbers of parvalbumin-immunoreactive neurons, whereas this layer is generally devoid of neurofilament

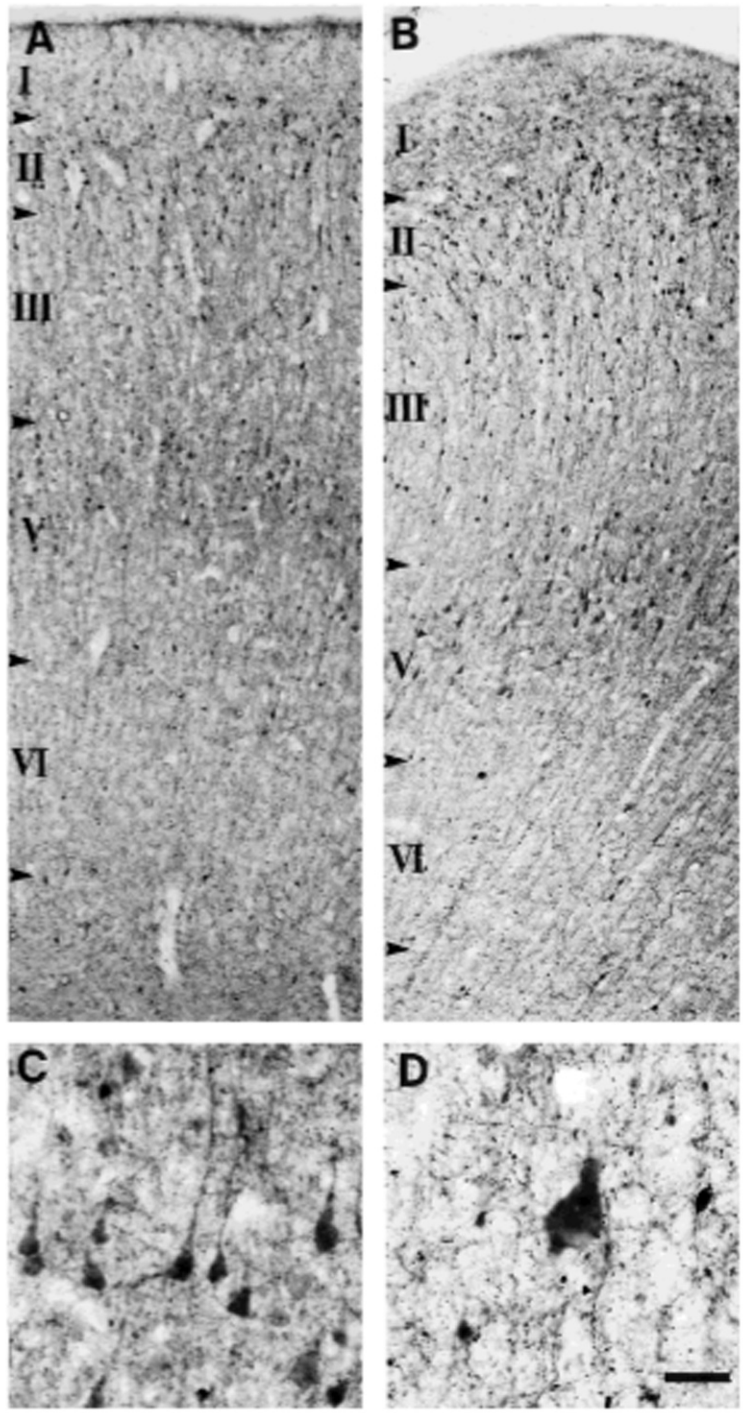

Fig. 13. Distribution of calretinin immunoreactivity in areas 25 **(A)** and 24a **(B)** of the human cingulate gyrus. Immunoreactive nonpyramidal neurons are most abundant in both areas in layer II and the superficial portion of layer III. Most resemble double bouquet neurons and have dendritic arbors oriented radially in the cortex. These areas also contain the highest density of calretinin-immunoreactive pyramidal neurons, which are found largely in layer V. Examples of these neurons are shown in **(C)**. A very large calretinin-immunoreactive neuron in area 24c'g, presumably one of the gigantopyramidal neurons that characterize this area is shown in **(D)**. Scale bar = 150 μm in A,B and 40 μm in C,D.

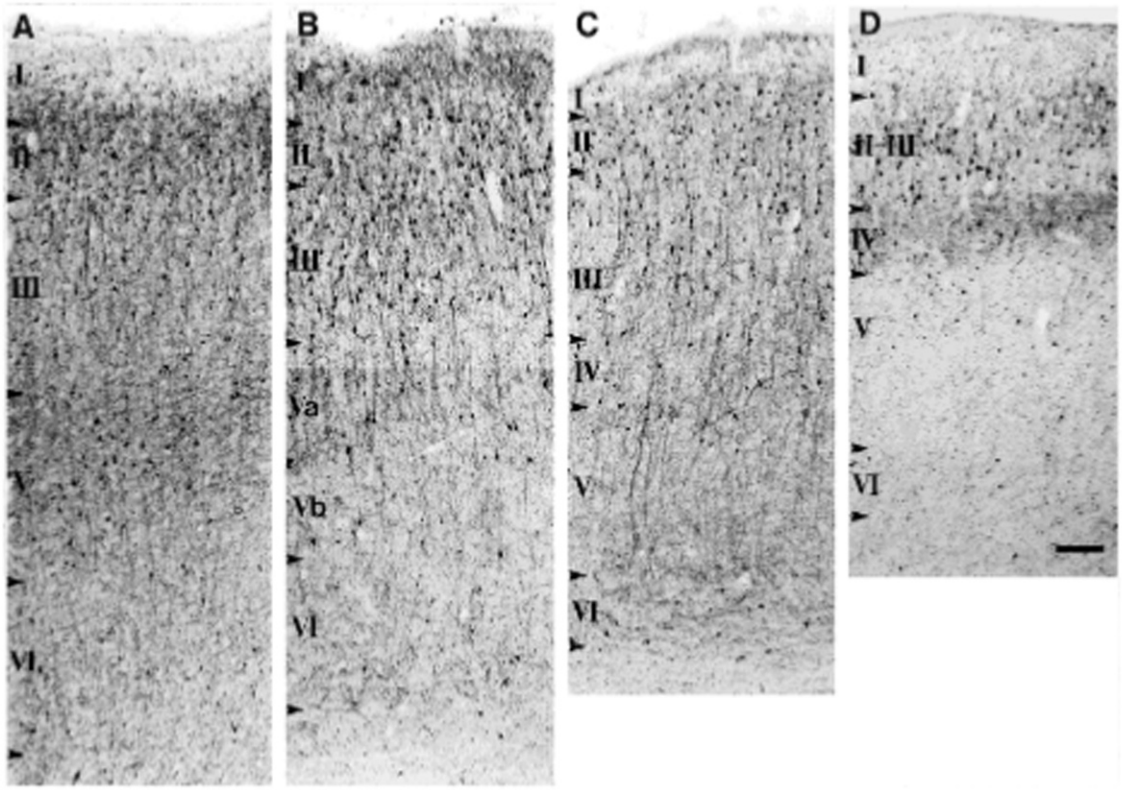

Fig. 14. Distribution of calretinin immunoreactivity in areas 24c **(A)**, 24c' **(B)**, 23b **(C)**, and 29 **(D)** of the human cingulate gyrus. In all these areas, calretinin-immunoreactive pyramidal neurons are found mostly in layer II and the superficial portion of layer III. Note the presence of calretinin-immunoreactive pyramidal neurons in layer V of area 24c (arrows in A) and their absence in areas 24c' and 23b. Area 29 contains somewhat fewer immunoreactive nonpyramidal neurons than the other areas, and is distinguished by a band of immunoreactivity in layer IV. Scale bar = 150 μm.

protein-containing neurons. One unusual finding is the presence in layers V and VI of large numbers of parvalbumin-immunoreactive structures that may represent the cartridges of chandelier neurons. Similar findings have been recently described (Kalus and Senitz, 1996). These structures represent the terminations of chandelier neurons along the axon initial segment of pyramidal neurons, and as such, signify a powerful inhibitory influence on pyramidal neuron firing. They have been described elsewhere in the monkey and human cerebral cortex, but they are usually located preferentially in superficial layers (DeFelipe et al., 1989; Lewis and Lund, 1990; Williams et al., 1992). An exception was a study in the human temporal neocortex that found a higher density of parvalbumin-immunoreactive cartridges in layers IV through VI than in layers II and III. In that study, which demonstrated a close association between parvalbumin-immunoreactive chandelier neurons and neurofilament protein-immunoreactive pyramidal neurons, it was suggested that the predominance of cartridges in superficial layers represented an association of this form of inhibitory control with corticocortically projecting neurons (Del Río and DeFelipe, 1994). The findings reported in the present study are in accord with this concept, since in the anterior portions of the primate cingulate gyrus, corticocortically projecting neurons take origin preferentially in deep cortical layers (Barbas, 1986; Hof et al., 1995b; Nimchinsky et al., 1993, 1996). Thus the presence of neurofilament protein-containing pyramidal neurons and of parvalbumin-immunoreactive chandelier neurons and their cartridges in deep layers in the anterior portions of the cingulate gyrus suggest that this location as the preferred site of origin of corticocortical projections in the human as well.

Calbindin-immunoreactive nonpyramidal neurons in macaque monkey and human have a relatively consistent pattern of distribution throughout the cingulate gyrus (Hof and Nimchinsky, 1992; Gabbott and Bacon, 1996b; the present study). Calbindin-immunoreactive pyramidal neurons, in contrast, are much more frequent in anterior than in posterior portions of the cingulate gyrus. This observation is similar to that described in the monkey cingulate cortex (Hof and Nimchinsky, 1992). Comparable heterogeneities in the distribution of these neurons have been reported in the visual areas of the temporal lobe (Kondo et al., 1994). Both the temporal lobe and the cingulate gyrus are characterized by progressive cytoarchi-

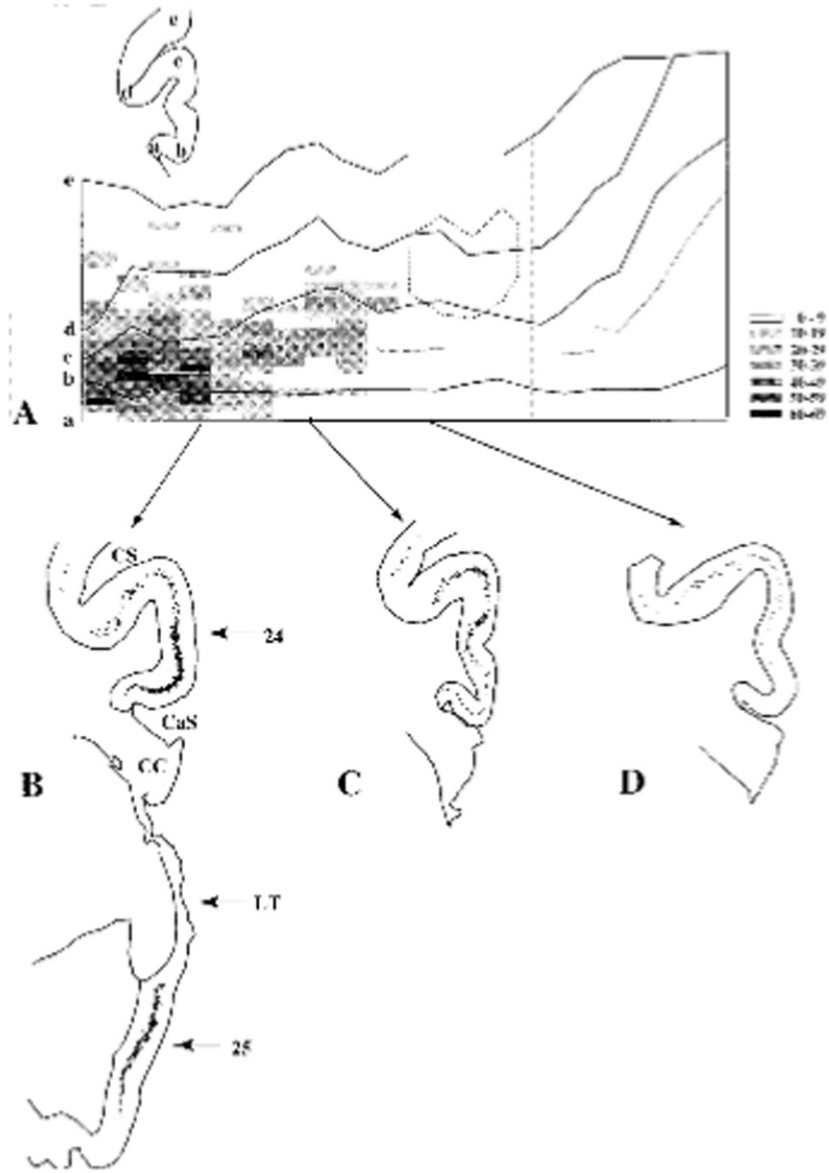

Fig. 15. **A**: Flattened representation of the human anterior cingulate cortex showing the semi-quantitative distribution of layer V calretinin-immunoreactive pyramidal-like neurons. The gigantopyramidal field (area 24c'g) is outlined with dotted lines, and a vertical broken line indicates the border between areas 24 and 23 as determined using the Nissl stain. Note that calretinin-immunoreactive pyramidal neurons are found largely in the most anterior and ventral portions of the cingulate gyrus. Elsewhere, they are scattered, mostly in the ventral bank of the cingulate sulcus. They are also found in densities comparable to area 24 in area 25, which is not included in this representation. **B–D**: Computer generated map of three coronal sections through areas 25 and 24 showing the distribution of calretinin-immunoreactive pyramidal-like neurons. Neurons were counted in 100 μm-wide bins and their local densities are coded in gray scale. The three sections shown here are 1.5 cm apart from each other. Although, as a result of their low density, they do not appear on the flattened map, CR-immunoreactive pyramidal-like neurons are found sporadically throughout area 24, and only disappear completely in area 23. CaS, callosal sulcus; CC, corpus callosum; CS, cingulate sulcus; LT, lamina terminalis. The position of the sulcal and gyral landmark lines on the flattened map (**a–e**) is indicated in the inset on top of panel A. See Figure 9A for cytoarchitectural boundaries among cingulate cortex subareas.

tectonic changes, with the anterior portions of each described as "dysgranular" or "agranular" for, among other characteristics, lacking a well-defined layer IV, and their posterior portions "isocortical", containing six well-defined cortical layers (Galaburda and Pandya, 1983; Pandya and Yeterian, 1985). In dysgranular parts of both cingulate gyrus and the temporal lobe, there were more calbindin-immunoreactive pyramidal neurons in layers II and III. In addition, the dysgranular and agranular regions are characterized by a considerable reduction in the number of parvalbumin-immunoreactive neurons (Kondo et al., 1994). These two populations of neurons, of course, represent functionally distinct classes, and the significance of the expression or lack of expression of a calcium-binding protein is still unclear. One possibility is suggested by the observation that the rostral portions of the temporal lobe and of the cingulate cortex represent two of the few cortical regions known to project directly to the amygdala. In both cases, the neurons furnishing this projection are found mostly, if not exclusively, in layer III (Aggleton et al., 1980). The calbindin-containing pyramidal neurons are thus positioned to participate in this projection. However, the more common role of layer III neocortical neurons, the furnishing of corticocortical projections, remains a distinct possibility (Jones, 1984). Nonetheless, such recurring gradients in different regions of the brain suggest that cytoarchitectonic variations may represent more than merely alternate shuffling of the same cell types found throughout the cortex.

Calretinin-immunoreactive nonpyramidal neurons populate superficial layers preferentially, as described both for the cingulate cortex in the monkey and other cortical regions in the monkey and human (Hof et al., 1993a,b; Condé et al., 1994). This pattern varies little through the numerous different cingulate cortical regions examined in the present study. However, the presence and distribution of calretinin-containing pyramidal-like neurons set the cingulate cortex apart from other cortical areas. While it was not possible in the present study to unambiguously identify these neurons as pyramidal neurons, as a result of their relatively light labeling that was usually restricted to the soma, a number of features suggest that they may, indeed, be pyramidal neurons. First, their overall morphology is unambiguously pyramidal, in layers that are dominated by this cell type. Second, their labeling is qualitatively different from that seen in the nonpyramidal neurons, which are labeled very intensely, throughout their cytoplasm, suggesting that they may belong to a completely different cell class. This is in contrast to the pyramidal-like neurons described by Condé et al. (1994) in the macaque monkey prefrontal cortex, which were well enough labeled to follow their dendrites for considerable distances. Finally, calcium-binding protein-containing pyramidal neurons are not without precedent, as calretinin is found in a subgroup of Betz cells in the human (Nimchinsky et al., 1992), parvalbumin is present in layer V pyramidal neurons in primate sensory and motor cortex (Preuss and Kaas, 1996), and in CA1 pyramidal neurons in the dog (Hof et al., 1996), and calbindin-containing pyramidal neurons populate layers II and III in many cortical areas in both the monkey and human (Hof and Morrison, 1991; Ferrer et al., 1992; Hof and Nimchinsky, 1992; Kondo et al., 1994; present study). However, until retrograde labeling or Golgi staining in the human is combined with immunocytochemistry, this question may remain unanswered, since comparable neurons are not observed in the nonhuman primate.

Regardless of the cell type to which calretinin-immunoreactive pyramidal-like neurons belong, they are restricted to the cingulate gyrus in general, and to areas 32, 25, 24, 24′, and 29 in particular, and this suggests a unique functional role. Their unusual nature is underscored by the fact that they are not seen in the human orbitofrontal cortex, a region that bears numerous cyto-and chemoarchitectonic similarities to the cingulate cortex (Hof et al., 1995). Calretinin-immunoreactive pyramidal neurons have been described in the newborn rat, but they disappear early in postnatal life (Vogt Weisenhorn et al., 1994; Fonseca et al., 1995; Schierle et al., 1997). It is possible that in the human cingulate cortex, these particular neurons continue to express this protein throughout life. These neurons appear to be a characteristic feature of the cingulate cortex, and are useful in the parcellation of these areas. The localization of these neurons almost exclusively in layer V does not help to define their connectivity, since this layer in the nonhuman primate gives rise not only to striatal and spinal cord projections, but also to corticocortical and corticopontine projections, as mentioned above (Barbas, 1986; Hutchins et al., 1988; Dum and Strick, 1991, 1992; Van Hoesen et al., 1993; Kunishio and Haber, 1994; He et al., 1995). It is notable, however, that the distribution of this cell type overlaps extensively, at the species level, and on a regional and laminar basis, with that of the spindle neurons that characterize these areas in the human (Nimchinsky et al., 1995). Unusual cell types, then, appear with much greater than average frequency in these parts of the human neocortex, and may represent a local neuronal specialization unique to the human brain.

Calcium-binding protein immunoreactivity defines distinctive neuropil staining patterns in the monkey and human cingulate cortex

With parvalbumin immunoreactivity, three separate gradients were observed. One consisted of the sheet-like labeling of the neuropil of layer III which began rostrally in the dorsolateral portions of the cingulate gyrus, and which gradually extended caudally, medially and ventrally, eventually to label layer III throughout the gyrus. Another consisted of the discrete labeling of the neuropil of areas 24a′ and 23a, which marked these areas in layers II through V. The third was the labeling of layer IV, wherever present. The combination of these three labeling patterns in cingulate cortex gives rise to a complex staining pattern, which in many respects resembled that of the monkey (Hof and Nimchinsky, 1992). Unlike the case in the monkey, calbindin immunoreactivity gave rise to staining patterns that resembled those found with parvalbumin, especially the first two patterns described above. In area 29, a slightly increased density of calbindin-immunoreactive neurons is observed in layer IV, but, in contrast with the pattern in the macaque monkey, no increase in neuropil labeling intensity characterizes area 29 or 30. Calretinin, however, with the exception of the immunoreactive band in areas 29 and 30, exhibited only minor changes in neuropil labeling along the cingulate gyrus. The sources of these labeling patterns are unclear. Some is clearly due to the immunoreactive nonpyramidal neurons that populate these areas. This is most likely the explanation for the patches in layer V of areas 24 and 24′, which correlate well

with layer Vb pyramidal and spindle neurons in these areas (Vogt et al., 1995). The concentration of immunoreactive terminals in the immediate vicinity of a certain cell population indicates a differential distribution of inhibitory control. For instance, the somata and proximal dendrites of layer Vb neurons appear to be surrounded by the presumably inhibitory terminals of parvalbumin- and calbindin-immunoreactive basket and possibly double bouquet cells. Layer Va neurons in the anterior cingulate cortex, in contrast, appear to be removed from such structures. It is possible that the neurons in this sublayer, which are notable for being particularly dense in the cingulate cortex, are subject to the inhibitory control of a discrete population of neurons which do not appear with any of the antibodies used in the present study, or are modulated not by terminals surrounding their somata, but by influences located more distally located on the dendritic arbor.

The dense and very intense labeling in the deep portion of layer III and of layer IV seen with antibodies to parvalbumin and calbindin may be due to labeled thalamocortical terminals. The three calcium-binding proteins examined in the present study are known to be present in various thalamic projection neurons in the rodent and nonhuman primate (Stichel et al., 1987; Celio, 1990; DeFelipe and Jones, 1991; Hashikawa et al., 1991; Jacobowitz and Winsky, 1991; Rausell et al., 1992a,b; Résibois and Rogers, 1992; Diamond et al., 1993; Arai et al., 1994). Since these are soluble proteins, they are distributed throughout the cytosplasm, and are thus present in the terminal fields of the thalamocortical neurons that contain them. This in turn gives rise to distinctive cortical labeling patterns (DeFelipe and Jones, 1991; Del Río and DeFelipe, 1994). Thus, the parvalbumin-immunoreactive band in the deep portion of layer III may derive from a projection from the mediodorsal nucleus, which projects to this layer and area in the macaque monkey (Giguère and Goldman-Rakic, 1988) and which contains numerous parvalbumin-immunoreactive neurons in the human thalamus (E.A. Nimchinsky, unpublished observations). The other major site of parvalbumin neuropil immunoreactivity, including all of area 23a and a considerable extent of area 23b, appears to coincide well with the regions in the monkey that receive projections from the medial pulvinar nucleus (Baleydier and Mauguière, 1985, 1987), which is also characterized in the human by parvalbumin immunoreactivity (E.A. Nimchinsky, unpublished observations). Similarly, the calretinin-immunoreactive band in areas 29 and 30, previously described in the macaque monkey (Hof and Nimchinsky, 1992) may derive from a thalamocortical projection from the laterodorsal nucleus, which projects to this layer in the macaque monkey and which, in the human, contains calretinin-immunoreactive neurons (Bentivoglio et al., 1993; Vogt et al., 1993). Of course, other structures project upon the cingulate cortex, such as the amygdala, but these projections do not have the particular regional and laminar characteristics expressed by the neuropil staining patterns described here (Porrino et al., 1981).

Functional implications

The cingulate motor areas. A recent study in the macaque monkey combining retrograde transport and immunocytochemistry demonstrated the utility of neurofilament protein as a marker for the cingulate motor areas (Nimchinsky et al., 1996). In particular, the appearance of immunoreactive neurons in layer III and a broad layer VI indicated the presence of the rostral cingulate motor area, CMAr, and the increased density of these neurons signalled the presence of the caudal cingulate motor area, CMAc. The subsequent lower density and thinning of layer VI, in addition to the presence of layer IV on the Nissl stain, indicated area 23, which was located caudally to the motor areas. In the monkey, these changes are relatively obvious, since the density of these neurons is significantly lower than in the human. Based on overall patterns, and by analogy to the nonhuman primate, it may be possible to approximate the locations of the human cingulate motor areas, with the CMAr located where the neurofilament protein-immunoreactive neurons first appear, and the CMAc located caudal to this area, and rostral to area 23. This represents a fairly large area of cortex, occupying roughly the middle third of the gyrus, but one that is proportional to the size of these areas in the macaque, and which agrees with the functional localization of these areas in the human (Grafton et al., 1993). Another potential clue is the calretinin-immunoreactive pyramidal neurons in layer V in the gigantopyramidal fields which were described by the Braaks (1976). The significance of calretinin immunoreactivity is that outside of the cingulate cortex, the only areas in the human cerebral cortex that have been described as containing calretinin-immunoreactive pyramidal neurons is the primary motor cortex, where a subpopulation of Betz cells contains calretinin (Nimchinsky et al., 1992), and the entorhinal cortex that contains a population of layer V calretinin-immunoreactive pyramidal cells (Nimchinsky and Morrison, unpublished observations). While not confirming a motor role, this represents another similarity between these neurons and the giant cells of Betz in the primary motor cortex. It is possible, then, that like the giant layer V cells of the primary motor cortex, some of the large pyramidal neurons in the cingulate cortex may be involved in motor function. In fact, it has been proposed that the gigantopyramidal area coincides, at least in part, to the cingulate motor areas described in the nonhuman primate (Dum and Strick, 1991, 1992, 1993). The present study lends further support to this hypothesis.

Other functions of the cingulate cortex. In addition to somatomotor function, numerous functions have been ascribed, completely or in part, to the cingulate gyrus in the human. (For review, see Devinsky et al., 1995.) These include autonomic (Pool and Ransohoff, 1949; Pool, 1954) and oculomotor (Talairach et al., 1973; Petit et al., 1993) functions, sensory functions, including pain processing (Foltz and White, 1962; Talbot et al., 1991; Rosen et al., 1994, Vogt et al., 1996), response selection (Petersen et al., 1988), and the manifestation of emotion (Hausser-Hauw and Bancaud, 1987; Arroyo et al., 1993). The present study suggests some possible anatomic correlates for some of these functions. For instance, one feature that appears fairly specific to the cingulate cortex is calretinin-immunoreactive pyramidal neurons in layer V. These are found almost exclusively in the anterior portions of the cingulate gyrus, and are most numerous in areas 25 and 24. The region thus delineated corresponds closely to the areas whose stimulation gives rise to autonomic effects and vocalization in both macaque monkey and human (Smith, 1945; Pool and Ransohoff, 1949; Kaada, 1951; Pool, 1954; Showers and Crosby, 1958; Dua and MacLean, 1964; Robinson and Mishkin, 1968; Jürgens and Ploog, 1970;

Jürgens, 1983). Studies that have analyzed other systems, such as response selection, spatial memory and selective attention have used functional imaging techniques, whose resolution limited the precise localization of function (Petersen et al., 1988; Pardo et al., 1990; Corbetta et al., 1991; Deiber et al., 1991; Bench et al., 1993; Hsieh et al., 1994; Lang et al., 1994; Larrue et al., 1994; Raichle et al., 1994). However, the consensus appears to be that these roles are subserved by cortical regions in the anterior half of the cingulate gyrus. Interestingly, this region is characterized by lower numbers of parvalbumin- and neurofilament protein-immunoreactive neurons, and greater numbers of calbindin-immunoreactive pyramidal neurons.

It is of note that none of the cytoarchitectonic regions described in the present study is delineable by sharp chemoarchitectonic borders, a fact that must be borne in mind when attempting to assign a cortical area to a region of functional activation. The anatomic boundaries in the cingulate gyrus may best be described as areas of transition from one staining pattern to another. The neuropil staining patterns, in particular, vary largely independently of cytoarchitecture. It would not be surprising, therefore, to find that the same holds true for the functional divisions of the human cingulate cortex. Further studies using markers with connectional or physiological significance may thus prove more practical than cytoarchitecture alone for the functional parcellation of this complex cortical region.

ACKNOWLEDGMENTS

We thank L.J. Vogt for expert technical assistance, R.S. Woolley and W.G.M Janssen for professional help with photography and computer graphics, Dr W.G. Young for software development, and Drs C. Bouras, D.P. Perl, and R. Insausti for providing some of the post-mortem materials used in this study.

LITERATURE CITED

Aggleton, J.P., M.J. Burton, and R.E. Passingham (1980) Cortical and subcortical afferents to the amygdala of the Rhesus monkey (*Macaca mulatta*). Brain Res. *190*:347–368.

Arsé, R., D.M. Jacobowitz, and S. Deura (1994) Distribution of calretinin, calbindin-D28k, and parvalbumin in the rat thalamus. Brain Res. Bull. *33*:595–614.

Arroyo, S., R.P. Lesser, B. Gordon, S. Uematsu, J. Hart, P. Schwerdt, K. Andreasson, and R.S. Fisher (1993) Mirth, laughter and gelastic seizures. Brain *116*:757–780.

Baleydier, C., and F. Mauguière (1985) Anatomical evidence for medial pulvinar connections with the posterior cingulate cortex, the retrosplenial area, and the posterior parahippocampal gyrus in monkeys. J. Comp. Neurol. *232*:219–228.

Baleydier, C., and F. Mauguière (1987) Network organization of the connectivity between parietal area 7, posterior cingulate cortex and medial pulvinar nucleus: A double fluorescent tracer study in monkey. Exp. Brain Res. *66*:385–393.

Barbas, H. (1986) Pattern in the laminar origin of corticocortical connections. J. Comp. Neurol. *252*:415–422.

Bench, C.J., C.D. Frith, P.M. Grasby, K.J. Friston, E. Paulesu, R.S.J. Frackowiak, and R.J. Dolan (1993) Investigations of the functional anatomy of attention using the Stroop test. Neuropsychologia *31*:907–922.

Bentivoglio, M., K. Kultas-Ilinsky, and I. Ilinsky (1993) Limbic thalamus: Structure, intrinsic organization, and connections. In B. A. Vogt and M. Gabriel (eds): Neurobiology of Cingulate Cortex and Limbic Thalamus. Boston: Birkhäuser, pp. 71–122.

Bloom, F.E., W.G. Young, E.A. Nimchinsky, P.R. Hof, and J.H. Morrison (1997) Neuronal vulnerability and informatics in human disease. In S.H. Koslow and M.F. Huerta (eds): Neuroinformatics—An Overview of the Human Brain Project, Progress in Neuroinformatics Research, Vol. 1. Mahwah, NJ: Lawrence Erlbaum, pp. 83–123.

Blümke, I., P.R. Hof, J.H. Morrison, and M.R. Celio (1990) Distribution of parvalbumin immunoreactivity in the visual cortex of Old World monkeys and humans. J. Comp. Neurol. *301*:417–432.

Blümke, I., P.R. Hof, J.H. Morrison, and M.R. Celio (1991) Parvalbumin in the monkey striate cortex: A quantitative immunoelectron-microscopy study. Brain Res. *554*:237–243.

Blümcke, I., E. Werunga, S. Kuzan, A.E. Hendrickson, and M.R. Celio (1994) Discrete reduction patterns of parvalbumin and calbindin D-28k immunoreactivity in the dorsal lateral geniculate nucleus and the striate cortex of adult macaque monkeys after monocular enucleation. Vis. Neurosci. *11*:1–11.

Braak, H. (1976) A primitive gigantopyramidal field buried in the depth of the cingulate sulcus of the human brain. Brain Res. *109*:219–233.

Braak, H. (1979a) Pigment architecture of the human telencephalic cortex IV. Regio retrosplenialis. Cell Tissue Res. *204*:431–440.

Braak, H. (1979b) Pigment architecture of the human telencephalic cortex V. Regio anterogenualis. Cell Tissue Res. *204*:441–451.

Braak, H., and E. Braak (1976) The pyramidal cells of Betz within the cingulate and precentral gigantopyramidal field in the human brain. Cell Tissue Res. *172*:103–119.

Brodmann, K. (1909) Vergleichende Lokalisationslehre der Grosshirnrinde in ihren Prinzipien dargestellt auf Grund des Zellenbaues. Leipzig: Barth. [Translated version: Garey, L.J. (1994) *Brodmann's* "Localisation in the cerebral cortex". London: Smith-Gordon.]

Campbell, M.J., and J.H. Morrison (1989) Monoclonal antibody to neurofilament protein (SMI-32) labels a subpopulation of pyramidal neurons in the human and monkey neocortex. J. Comp. Neurol. *282*:191–205.

Carmichael, S.T., and J.L. Price (1994) Architectonic subdivision of the orbital and medial prefrontal cortex in the macaque monkey. J. Comp. Neurol. *346*:366–402.

Celio, M.R. (1990) Calbindin D-28k and parvalbumin in the rat nervous system. Neuroscience *35*:375–475.

Celio, M.R., W. Baier, P. De Viragh, E. Schärer, and C. Gerday (1988) Monoclonal antibodies directed against the calcium binding protein parvalbumin. Cell Calcium *9*:81–89.

Celio, M.R., W. Baier, H.G. Gregersen, P.A. De Viragh, L. Schärer, and A.W. Norman (1990) Monoclonal antibodies to calbindin D-28k. Cell Calcium *11*:599–602.

Condé, F., J.S. Lund, D.M. Jacobowitz, K.G. Baimbridge, and D.A. Lewis (1994) Local circuit neurons immunoreactive for calretinin, calbindin D-28k or parvalbumin in monkey prefrontal cortex: Distribution and morphology. J. Comp. Neurol. *341*:95–116.

Corbetta, M., F.M. Miezin, S. Dobmeyer, G.L. Shulman, and S.E. Petersen (1991) Selective and divided attention during visual discriminations of shape, color, and speed: Functional anatomy by positron emission tomography. J. Neurosci. *11*:2383–2402.

DeFelipe, J., S.H.C. Hendry, and E.G. Jones (1989) Visualization of chandelier cell axons by parvalbumin immunoreactivity in monkey cerebral cortex. Proc. Natl. Acad. Sci. USA *86*:2093–2097.

DeFelipe, J., and E.G. Jones (1991) Parvalbumin immunoreactivity reveals layer IV of monkey cerebral cortex as a mosaic of microzones of thalamic afferent terminations. Brain Res. *562*:39–47.

DeFelipe, J., and E.G. Jones (1992) High-resolution light and electron microscopic immunocytochemistry of colocalized GABA and calbindin D-28k in somata and double bouquet cell axons of monkey somatosensory cortex. Eur. J. Neurosci. *4*:46–60.

Deiber, M.P., R.E. Passingham, J.G. Colebatch, K.J. Friston, P.D. Nixon, and R.S.J. Frackowiak (1991) Cortical areas and the selection of movement: A study with positron emission tomography. Exp. Brain Res. *84*:393–402.

Del Río, M.R., and J. DeFelipe (1994) A study of SMI32-stained pyramidal cells, parvalbumin-immunoreactive chandelier cells and presumptive thalamocortical axons in the human temporal neocortex. J. Comp. Neurol. *342*:389–408.

Devinsky, O., M.J. Morrell, and B.A. Vogt (1995) Contributions of anterior cingulate cortex to behaviour. Brain *118*:279–306.

Diamond, I.T., D. Fitzpatrick, and D. Schmechel (1993) Calcium binding proteins distinguish large and small cells of the ventral posterior and lateral geniculate nuclei of the prosimian galago and the tree shrew (*Tupaia belangeri*). Proc. Natl. Acad. Sci. USA *90*:1425–1429.

Dua, S., and P.D. MacLean (1964) Localization for penile erection in medial frontal lobe. Am. J. Physiol. *207*:1425–1434.

Dum, R.P., and P.L. Strick (1991) The origin of corticospinal projections from the premotor areas in the frontal lobe. J. Neurosci. *11*:667–689.

Dum, R.P., and P.L. Strick (1992) Medial wall motor areas and skeletomotor control. Curr. Opin. Neurobiol. 2:836–839.

Dum, R.P., and P.L. Strick (1993) Cingulate motor areas. In B.A. Vogt and M. Gabriel (eds): Neurobiology of Cingulate Cortex and Limbic Thalamus. Boston, MA: Birkhäuser, pp. 415–441.

Ferrer, I., T. Tuñon, E. Soriano, A. del Río, I. Iraizoz, M. Fonseca, and N. Guionnet (1992) Calbindin immunoreactivity in normal human temporal neocortex. Brain Res. *572*:33–41.

Foltz, E.L., and L.E. White Jr. (1962) Pain "relief" by frontal cingulumotomy. J. Neurosurg. *19*:83–100.

Fonseca, M., J.A. Del Río, A. Martínez, S. Gómez, and E. Soriano (1995) Development of calretinin immunoreactivity in the neocortex of the rat. J. Comp. Neurol. *361*:177–192.

Gabbott, P.L.A., and S.J. Bacon (1996a) Local circuit neurons in the medial prefrontal cortex (areas 24a,b,c, 25 and 32) in the monkey: I. Cell morphology and morphometrics. J. Comp. Neurol. *364*:567–608.

Gabbott, P.L.A., and S.J. Bacon (1996b) Local circuit neurons in the medial prefrontal cortex (areas 24a,b,c, 25 and 32) in the monkey: II. Quantitative areal and laminar distributions. J. Comp. Neurol. *364*:609–636.

Giguère, M., and P.S. Goldman-Rakic (1988) Mediodorsal nucleus: Areal, laminar, and tangential distribution of afferents and efferents in the frontal lobe of Rhesus monkeys. J. Comp. Neurol. *277*:195–213.

Grafton, S.T., R.P. Woods, and J.C. Mazziotta (1993) Within-arm somatotopy in human motor areas determined by positron emission tomography imaging of cerebral blood flow. Exp. Brain Res. *95*:172–176.

Hashikawa, T., E. Rausell, M. Molinari, and E.G. Jones (1991) Parvalbumin- and calbindin-containing neurons in the monkey medial geniculate complex: Differential distribution and cortical layer specific projections. Brain Res. *544*:335–341.

Hausser-Hauw, C., and J. Bancaud (1987) Gustatory hallucinations in epileptic seizures. Brain *110*:339–359.

He, S.Q., R.P. Dum, and P.L. Strick (1995) Topographic organization of corticospinal projections from the frontal lobe: Motor areas on the medial surface of the hemisphere. J. Neurosci. *15*:3284–3306.

Hof, P.R., and J.H. Morrison (1991) Neocortical neuronal subpopulations labeled by a monoclonal antibody to calbindin exhibit differential vulnerability in Alzheimer's disease. Exp. Neurol. *111*:293–301.

Hof, P.R., and J.H. Morrison (1995) Neurofilament protein defines regional patterns of cortical organization in the macaque monkey visual system: A quantitative immunohistochemical analysis. J. Comp. Neurol. *352*: 161–186.

Hof, P.R., and E.A. Nimchinsky (1992) Regional distribution of neurofilament and calcium-binding proteins in the cingulate cortex of the macaque monkey. Cereb. Cortex 2:456–467.

Hof, P.R., E.J. Mufson, and J.H. Morrison (1995a) The human orbitofrontal cortex: cytoarchitecture and quantitative immunohistochemical parcellation. J. Comp. Neurol. *359*:48–68.

Hof, P.R., E.A. Nimchinsky, and J.H. Morrison (1995b) Neurochemical phenotype of corticocortical connections in the macaque monkey: Quantitative analysis of a subset of neurofilament protein-immunoreactive projection neurons in frontal, parietal, temporal, and cingulate cortices. J. Comp. Neurol. *362*:109–133.

Hof P.R., R.E. Rosenthal, and G. Fiskum (1996) Distribution of neurofilament protein and calcium-binding proteins parvalbumin, calbindin, and calretinin in the canine hippocampus. J. Chem. Neuroanat. *11*:1–12.

Hof, P.R., H.-J. Lüth, J.H. Rogers, and M.R. Celio (1993a) Calcium-binding proteins define subpopulations of interneurons in the cingulate cortex. In B.A. Vogt and M. Gabriel (eds): Neurobiology of Cingulate Cortex and Limbic Thalamus. Boston, MA: Birkhäuser, pp. 181–205.

Hof, P.R., E.A. Nimchinsky, M.R. Celio, C. Bouras, and J.H. Morrison (1993b) Calretinin-immunoreactive neocortical interneurons are unaffected in Alzheimers disease. Neurosci. Lett. *152*:145–149.

Haish, J.-C., Ö. Hägermark, M. Stähle-Bäckdahl, K. Ericson, L. Eriksson, S. Stens-Ekander, and M. Ingvar (1994) Urge to scratch represented in the human cerebral cortex during itch. J. Neurophysiol. *72*:3004–3008.

Hutchins, K.D., A.M. Martino, and P.L. Strick (1988) Corticospinal projections from the medial wall of the hemisphere. Exp. Brain Res. *71*:667–672.

Jacobowitz, D.M., and L. Winsky (1991) Immunocytochemical localization of calretinin in the forebrain of the rat. J. Comp. Neurol. *304*:198–218.

Jones, E.G. (1984) Laminar distribution of cortical efferent cells. In A. Peters and E. G. Jones (eds): Cerebral Cortex, Vol. 1, Cellular Components of the Cerebral Cortex. New York: Plenum Press, pp. 521–553.

Jones, E.G., E. Dell'Anna, M. Molinari, E. Rausell, and T. Hashikawa (1995) Subdivisions of macaque monkey auditory cortex revealed by calcium-binding protein immunoreactivity. J. Comp. Neurol. 362:1–19.

Jürgens, U. (1983) Afferent fibers to the cingular vocalization region in the squirrel monkey. Exp. Neurol. *80*:395–409.

Jürgens, U., and D. Ploog (1970) Cerebral representations of vocalization in the squirrel monkey. Exp. Brain Res. *10*:532–554.

Kahn, P., and D. Senitz (1996) Parvalbumin in the human anterior cingulate cortex: Morphological heterogeneity of inhibitory interneurons. Brain Res. *729*:65–54.

Kaada, B. (1951) Somato-motor, autonomic and electrocorticographic responses to electrical stimulation of rhinencephalic and other structures in primates, cat and dog. Acta Physiol. Scand. *24*:1–285.

Kondo, H., T. Hashikawa, K. Tanaka, and E.G. Jones (1994) Neurochemical gradient along the monkey occipito-temporal cortical pathway. NeuroReport *5*:613–616.

Kunishio, K., and S.N. Haber (1994) Primate cingulostriatal projection: Limbic striatal versus sensorimotor striatal input. J. Comp. Neurol. *350*:337–356.

Lang, W., L. Petit, P. Héllinger, U. Pietrzyk, N. Tzourio, B. Mazoyer, and A. Berthoz (1994) A positron emission tomography study of oculomotor imagery. NeuroReport *5*:921–924.

Larrue, V., P. Celsis, and A.M.-V. Bès J.P. (1994) The functional anatomy of attention in humans: Cerebral blood flow changes induced by reading, naming and the Stroop test. J. Cereb. Blood Flow Metab. *14*:958–962.

Lee, V.M.Y., L. Otvos Jr., M.J. Carden, M. Hollosi, B. Dietzschold, and R.A. Lazzarini (1988) Identification of the major multiphosphorylation site in mammalian neurofilaments. Proc. Natl. Acad. Sci. USA *85*:1998–2002.

Lewis, D.A., and J.S. Lund (1990) Heterogeneity of chandelier neurons in monkey neocortex: Corticotropin-releasing factor- and parvalbumin-immunoreactive populations. J. Comp. Neurol. 293:599–615.

Molinari, M., M.R. Dell'Anna, E. Rausell, M.G. Leggio, T. Hashikawa, and E.G. Jones (1995) auditory thalamocortical pathways defined in monkeys by calcium-binding protein immunoreactivity. J. Comp. Neurol. 362:171–194.

Morecraft, R.J., and G.W. Van Hoesen (1992) Cingulate input to primary and supplementary motor cortices in the rhesus monkey: Evidence for somatotopy in cingulate areas 24c and 23c. J. Comp. Neurol. 322:471–489.

Nimchinsky, E.A., P.R. Hof, N. Bross, S.W. Rogers, T. Moran, G.F. Gasic, S. Heinemann, and J.H. Morrison (1993) Glutamate receptor subunit and neurofilament protein immunoreactivities differentiate subsets of corticocortically projecting neurons in the monkey cingulate cortex. Soc. Neurosci. Abstr. *19*:473.

Nimchinsky, E.A., P.R. Hof, D.P. Perl, and J.H. Morrison (1992) The frontal cortex in neurodegenerative disorders: cellular and regional patterns of vulnerability. Soc. Neurosci. Abstr. *18*:557.

Nimchinsky, E.A., P.R. Hof, W.G. Young, and J.H. Morrison (1996) Neurochemical, morphologic, and laminar characterization of cortical projection neurons in the cingulate motor areas of the macaque monkey. J. Comp. Neurol. *374*:136–160.

Nimchinsky, E.A., B.A. Vogt, J.H. Morrison, and P.R. Hof (1995) Spindle neurons of the human anterior cingulate cortex. J. Comp. Neurol. 355:27–37.

Pandya, D.N., and E.H. Yeterian (1985) Architecture and connections of cortical association areas. In A. Peters and E.G. Jones (eds): Cerebral Cortex, Vol. 4, Association and Auditory Cortices. New York: Plenum Press, pp. 3–61.

Pardo, J.V., P.J. Pardo, K.W. Janer, and M.E. Raichle (1990) The anterior cingulate cortex mediates processing selection in the Stroop attentional conflict paradigm. Proc. Natl. Acad. Sci. USA *87*:256–259.

Petersen, S.E., P.T. Fox, M.I. Posner, M. Mintun, and M.E. Raichle (1988) Positron emission tomographic studies of the cortical anatomy of single-word processing. Nature *331*:585–589.

Petit, L., C. Orssaud, N. Tzourio, G. Salamon, B. Mazoyer, and A. Berthoz (1993) PET study of voluntary saccadic eye movements in humans: Basal ganglia-thalamocortical system and cingulate cortex involvement. J. Neurophysiol. 69:1009–1017.

Pool, J.L. (1954) The visceral brain of man. J. Neurosurg. *11*:45–63.

Pool, J.L., and J. Ransohoff (1949) Autonomic effects on stimulating the rostral portion of cingulate gyri in man. J. Neurophysiol. *12*:385–392.

Porrino, L., A.M. Crane, and P.S. Goldman-Rakic (1981) Direct and indirect pathways from the amygdala to the frontal lobe in Rhesus monkeys. J. Comp. Neurol. *198*:121–136.

Preuss, T.M., and J.H. Kaas (1996) Parvalbumin-like immunoreactivity of layer V pyramidal cells in the motor and somatosensory cortex of adult primates. Brain Res. *712*:353–357.

Raichle, M.E., J.A. Fiez, T.O. Videen, A.M.K. MacLeod, J.V. Pardo, P.T. Fox, and S.E. Petersen (1994) Practice-related changes in human brain functional anatomy during nonmotor learning. Cereb. Cortex *4*:8–26.

Ramsell, E., and E.G. Jones (1991a) Histochemical and immunocytochemical compartments of the thalamic VPM nucleus in monkeys and their relationship to the representational map. J. Neurosci. *11*:210–225.

Ramsell, E., and E.G. Jones (1991b) Chemically distinct compartments of the thalamic VPM nucleus in monkeys relay principal and spinal trigeminal pathways to different layers of the somatosensory cortex. J. Neurosci. *11*:226–237.

Ramsell, E., C.S. Rao, A. Viitanen, G.W. Huntley, and E.G. Jones (1992a) Calbindin and parvalbumin cells in monkey VPL thalamic nucleus: Distribution, laminar cortical projections, and relations to spinothalamic terminations. J. Neurosci. *12*:4088–4111.

Ramsell, E., C.G. Cusick, E. Taub, and E.G. Jones (1992b) Chronic deafferentation in monkeys differentially affects nociceptive and nonnociceptive pathways distinguished by specific calcium-binding proteins and down-regulates γ-aminobutyric acid type A receptors at thalamic levels. Proc. Natl. Acad. Sci. USA *89*:2571–2575.

Résibois, A., and J.H. Rogers (1992) Calretinin in rat brain: An immunohistochemical study. Neuroscience *46*:101–134.

Robinson, B.W., and M. Mishkin (1968) Penile erection evoked from forebrain structures in *Macaca mulatta*. Arch. Neurol. *19*:184–198.

Rose, M. (1927) Gyrus limbicus anterior und Regio retrosplenialis (Cortex holoprotoptychos quinquestratificatus)-Vergleichende Architektonik bei Tier und Menschen. J. Psychol. Neurol. *35*:5–217.

Rosen, S.D., E. Paulesu, C.D. Frith, R.S.J. Frackowiak, G.J. Davies, T. Jones, and P.G. Camici (1994) Central nervous pathways mediating angina pectoris. Lancet *344*:147–150.

Schierle, G.S., J.G. Gander, C. D'Orlando, M.R. Celio, and D.M. Vogt Weisenhorn (1997) Calretinin-immunoreactivity during postnatal development of the rat isocortex: A qualitative and quantitative study. Cereb. Cortex *7*:130–142.

Schwaller, B., P. Buchwald, I. Blümke, M.R. Celio, and W. Hunziker (1993) Characterization of a polyclonal antiserum against the purified human recombinant calcium binding protein calretinin. Cell Calcium *14*:639–648.

Showers, M.J.C., and E.C. Crosby (1958) Somatic and visceral responses from the cingulate gyrus. Neurology *8*:561–565.

Smith, W. (1945) The functional significance of the rostral cingular cortex as revealed by its responses to electrical excitation. J. Neurophysiol. *8*:241–255.

Sternberger, L.A., and N.H. Sternberger (1983) Monoclonal antibodies distinguish phosphorylated and nonphosphorylated forms of neurofilaments *in situ*. Proc. Natl. Acad. Sci. USA *80*:6126–6130.

Stichel, C.C., W. Singer, C.W. Heizman, and A.W. Norman (1987) Immunohistochemical localization of calcium-binding proteins, parvalbumin and calbindin-D 28k, in the adult and developing visual cortex of cats: A light and electron microscopic study. J. Comp. Neurol. *262*:563–577.

Talairach, J., J. Bancaud, S. Geier, M. Bordas-Ferrer, A. Bonis, G. Szikla, and M. Rusu (1973) The cingulate gyrus and human behavior. Electroenceph. Clin. Neurophysiol. *34*:45–52.

Talbot, J.D., S. Marrett, A.C. Evans, E. Meyer, M.C. Bushnell, and G.H. Duncan (1991) Multiple representations of pain in human cerebral cortex. Science *251*:1355–1358.

Van Hoesen, G.W., R.J. Morecraft, and B.A. Vogt (1993) Connections of the monkey cingulate cortex. In B.A. Vogt and M. Gabriel (eds): Neurobiology of Cingulate Cortex and Limbic Thalamus. Boston, MA: Birkhäuser, pp. 249–284.

Vogt, B.A. (1976) Retrosplenial cortex in the rhesus monkey: A cytoarchitectonic and Golgi study. J. Comp. Neurol. *169*:63–98.

Vogt, B.A. (1993) Structural organization of cingulate cortex: Areas, neurons, and somatodendritic transmitter receptors. In B.A. Vogt and M. Gabriel (eds): Neurobiology of Cingulate Cortex and Limbic Thalamus. Boston, MA: Birkhäuser, pp. 19–70.

Vogt, B.A., S. Derbyshire, and A.K.P. Jones (1996) Pain processing in four regions of human cingulate cortex localized with co-registered PET and MR imaging. Eur. J. Neurosci. *8*:1461–1473.

Vogt, B.A., E.A. Nimchinsky, J.H. Morrison, and P.R. Hof (1993) Calretinin may define thalamocortical connections between the human limbic thalamus and cingulate cortex. Soc. Neurosci. Abstr. *19*:1445.

Vogt, B.A., E.A. Nimchinsky, L.J. Vogt, and P.R. Hof (1995) Human cingulate cortex: Surface features, flat maps, and cytoarchitecture. J. Comp. Neurol. *359*:490–506.

Vogt, B.A., D.N. Pandya, and D.L. Rosene (1987) Cingulate cortex of the rhesus monkey: I. Cytoarchitecture and thalamic afferents. J. Comp. Neurol. *262*:256–270.

Vogt, B.A., R.W. Sikes, H.A. Swadlow, and T.G. Weyand (1986) Rabbit cingulate cortex: cytoarchitecture, physiological border with visual cortex, and afferent cortical connections of visual, motor, postauditory, and intracingulate origin. J. Comp. Neurol. *248*:74–94.

Vogt B.A., L.J. Vogt, E.A. Nimchinsky, and P.R. Hof (1997) Primate cingulate cortex: chemoarchitecture and its disruption in Alzheimer's disease. In F.E. Bloom, A. Björklund, T. Hökfelt (eds): Handbook of Chemical Neuroanatomy Vol. 13, The Primate Nervous System Part I. Amsterdam: Elsevier, pp. 453–526.

Vogt Weisenhorn, D.M., E. Werunga-Prieto, and M.R. Celio (1994) Localization of calretinin in cells of layer I (Cajal-Retzius cells) of the developing cortex of the rat. Brain Res. *82*:293–297.

Von Economo, C. (1927) L'Architecture Cellulaire Normale de l'Ecorce Cérébrale. Paris: Masson.

Williams, S.M., P.S. Goldman-Rakic, and C. Leranth (1992) The synaptology of parvalbumin-immunoreactive neurons in the primate prefrontal cortex. J. Comp. Neurol. *320*:353–369.

Young W.G., J.H. Morrison, P.R. Hof, E.A. Nimchinsky, and F.E. Bloom (1996) NeuroZoom—Topographical mapping and stereological counting, distribution of data, and collaborative computing. Soc. Neurosci. Abstr. *22*:1238.